NAVAL POSTGRADUATE SCHOOL

MONTEREY, CALIFORNIA

THESIS

TRANSIENT BEHAVIOR OF LIGHT-EMITTING ELECTROCHEMICAL CELLS

by

Yevtte A. Davis

June 2011

Thesis Co-Advisors: Peter P. Crooker
Nancy M. Haegel

Approved for public release; distribution is unlimited

THIS PAGE INTENTIONALLY LEFT BLANK

REPORT DOCUMENTATION PAGE			Form Approved OMB No. 0704-0188
Public reporting burden for this collection of information is estimated to average 1 hour per response, including the time for reviewing instruction, searching existing data sources, gathering and maintaining the data needed, and completing and reviewing the collection of information. Send comments regarding this burden estimate or any other aspect of this collection of information, including suggestions for reducing this burden, to Washington headquarters Services, Directorate for Information Operations and Reports, 1215 Jefferson Davis Highway, Suite 1204, Arlington, VA 22202-4302, and to the Office of Management and Budget, Paperwork Reduction Project (0704-0188) Washington DC 20503.			
1. AGENCY USE ONLY *(Leave blank)*	**2. REPORT DATE** June 2011	**3. REPORT TYPE AND DATES COVERED** Master's Thesis	
4. TITLE AND SUBTITLE Transient Behavior of Light-Emitting Electrochemical Cells		**5. FUNDING NUMBERS**	
6. AUTHOR(s) Yevtte A. Davis			
7. PERFORMING ORGANIZATION NAME(S) AND ADDRESS(ES) Naval Postgraduate School Monterey, CA 93943-5000		**8. PERFORMING ORGANIZATION REPORT NUMBER**	
9. SPONSORING /MONITORING AGENCY NAME(S) AND ADDRESS(ES) Technology Transition Initiative of the Office of the Director of Defense Research and Engineering (DDRE), National Science Foundation under grant DMR 0804527		**10. SPONSORING/MONITORING AGENCY REPORT NUMBER**	
11. SUPPLEMENTARY NOTES The views expressed in this thesis are those of the author and do not reflect the official policy or position of the Department of Defense or the U.S. Government. IRB Protocol number _____N/A_____.			
12a. DISTRIBUTION / AVAILABILITY STATEMENT Approved for public release; distribution is unlimited		**12b. DISTRIBUTION CODE**	

13. ABSTRACT (maximum 200 words)

Recent prototypes of the individual identification friend or foe (IIFF) patch use a light-emitting electrochemical cell (LEC) as the emitter. This research characterizes the transient behavior of LECs by measuring transient capacitance. The transient capacitance data are important to improve understanding of the underlying physics describing the operation of the LEC.

The research goal was to make the first transient measurements of an LEC's capacitance as a function of temperature and bias, while simultaneously measuring the transient light output and current, to monitor in-situ junction formation inside an LEC. Capacitance changes varying from 5-30 nF are measured, depending on applied voltage and device temperature. Strong temperature dependence of the rate of change of capacitance suggests Arrhenius-type behavior associated with ion motion with an activation energy of ~1.27 eV. The initial rate of change of capacitance is faster than the rate of change of light and current, suggesting that modification of the field near the contacts plays a key role in controlling free carrier injection. Initially capacitance increases monotonically upon application of bias, however, at longer times decreasing and even oscillating capacitance has been observed. This behavior provides new information on the dynamics of ion motion and carrier injection in LECs.

14. SUBJECT TERMS LEC, Transient, Capacitance, Junction, Arrhenius-type Behavior, Rate of Change, Ion Motion, Carrier Injection			**15. NUMBER OF PAGES** 81
			16. PRICE CODE
17. SECURITY CLASSIFICATION OF REPORT Unclassified	**18. SECURITY CLASSIFICATION OF THIS PAGE** Unclassified	**19. SECURITY CLASSIFICATION OF ABSTRACT** Unclassified	**20. LIMITATION OF ABSTRACT** UU

NSN 7540-01-280-5500 Standard Form 298 (Rev. 2-89)
Prescribed by ANSI Std. 239-18

THIS PAGE INTENTIONALLY LEFT BLANK

Approved for public release; distribution is unlimited

TRANSIENT BEHAVIOR OF LIGHT-EMITTING ELECTROCHEMICAL CELLS

Yevtte A. Davis
Lieutenant, United States Navy
B.S., Westminster College of Salt Lake City, 2005

Submitted in partial fulfillment of the
requirements for the degree of

MASTER OF SCIENCE IN PHYSICS

from the

NAVAL POSTGRADUATE SCHOOL
June 2011

Author: Yevtte A. Davis

Approved by: Peter P. Crooker
Thesis Co-Advisor

Nancy M. Haegel
Thesis Co-Advisor

Andres Larraza
Chair, Department of Physics

THIS PAGE INTENTIONALLY LEFT BLANK

ABSTRACT

Recent prototypes of the individual identification friend or foe (IIFF) patch use a light-emitting electrochemical cell (LEC) as the emitter. This research characterizes the transient behavior of LECs by measuring transient capacitance. The transient capacitance data are important to improve understanding of the underlying physics describing the operation of the LEC.

The research goal was to make the first transient measurements of an LEC's capacitance as a function of temperature and bias, while simultaneously measuring the transient light output and current, to monitor in-situ junction formation inside an LEC. Capacitance changes varying from 5-30 nF are measured, depending on applied voltage and device temperature. Strong temperature dependence of the rate of change of capacitance suggests Arrhenius-type behavior associated with ion motion with an activation energy of ~1.27 eV. The initial rate of change of capacitance is faster than the rate of change of light and current, suggesting that modification of the field near the contacts plays a key role in controlling free carrier injection. Initially capacitance increases monotonically upon application of bias, however, at longer times decreasing and even oscillating capacitance has been observed. This behavior provides new information on the dynamics of ion motion and carrier injection in LECs.

THIS PAGE INTENTIONALLY LEFT BLANK

TABLE OF CONTENTS

I. INTRODUCTION....1
A. MOTIVATION FOR DEVICE USE....1
B. MOTIVATION TO STUDY DEVICE....2
C. THESIS OVERVIEW....3

II. THEORIES OF OPERATION....5
A. CONSTRUCTION AND COMPOSITION OF LECS....5
B. GENERAL MODE OF OPERATION....7
C. THE ELECTROCHEMICAL MODEL....7
1. Anode....8
2. Cathode....8
D. THE ELECTRODYNAMIC MODEL....11
1. Anode....11
2. Cathode....11
E. A UNIFYING MODEL....13
F. APPLYING THE MODELS....14

III. EXPERIMENTAL SETUP AND DATA COLLECTION PROCESS....15
A. GENERAL EXPERIMENTAL SETUP....15
B. ELECTRICAL CONNECTIONS OF THE IFF LEC....16
C. COLLECTION OF LIGHT OUTPUT....17
D. TEMPERATURE CHAMBER....19
E. CURRENT SOURCE....20
F. VOLTAGE SOURCE....20
G. LABVIEW 8.6 PROGRAM OLED3....22
1. Model of the LEC....22
2. Calculating R, C and I....23

IV. TEMPERATURE DEPENDENT MEASUREMENTS....27
A. LEC TURN-ON TRANSIENTS....27
B. TEMERATURE DEPENDENCE OF CURRENT....27
C. CORRELATION BETWEEN CURRENT AND LIGHT OUTPUT....31
D. TEMPERATURE DEPENDENCE OF CAPACITANCE....34
E. RELATING CAPACITANCE, CURRENT AND LIGHT OUTPUT....40

V. VOLTAGE DEPENDENT MEASUREMENTS....45
A. LEC TURN-ON TRANSIENTS....45
B. VOLTAGE DEPENDENCE OF CURRENT....45
C. VOLTAGE DEPENDENCE OF LIGHT OUTPUT....47
D. VOLTAGE DEPENDENCE OF CAPACITANCE....50
E. RELATING CAPACITANCE, CURRENT AND LIGHT OUTPUT....53
F. TRANSIENT BEHAVIOR AS A FUNCTION OF VOLTAGE AT 22°C....56

VI. CONCLUSIONS AND SUGGESTIONS FOR FURTHER RESEARCH....61

A. SUMMARY OF RESULTS 61
B. SUGGESTIONS FOR FURTHER RESEARCH.....62
LIST OF REFERENCES.....63
INITIAL DISTRIBUTION LIST.....65
OLED3 PROGRAM BLOCK DIAGRAM ……SEE INSERT OR CLICK HERE

LIST OF FIGURES

Figure 1. IR Reflective Patch. 1
Figure 2. Planar LEC. 5
Figure 3. Sandwich LEC. 6
Figure 4. Chemical Structure of PPV. 6
Figure 5. Chemical Structure of PEO. 7
Figure 6. Electrochemical (EC) Model of P-N Junction Formation [From 6]. 9
Figure 7. Electric Field in EC Model. 9
Figure 8. Current-Light-Voltage Characteristics [From 7]. 10
Figure 9. Capacitance-Voltage and Current-Voltage Characteristics [From 10]. 10
Figure 10. Electrodynamic (ED) Model of Charge Diffusion [From 6]. 12
Figure 11. Electric Field in ED Model. 12
Figure 12. Mapping of Potential and Electric Field of LEC [From 13]. 13
Figure 13. General Experimental Setup. 15
Figure 14. LEC Devices. 16
Figure 15. LEC Connected to Daughter Board. 16
Figure 16. Schematic of LEC and Switch Wiring. 17
Figure 17. Schematic of Photodiode and DAQ Setup. 18
Figure 18. Cutoff Frequency Due to Capacitor. 19
Figure 19. Temperature Chamber. 20
Figure 20. Display of Agilent in R-X Mode. 21
Figure 21. LEC Electrical Model as Resistor and Capacitor in Parallel. 22
Figure 22. OLED3 Front Panel 25
Figure 23. Current as a Function of Time Following Application of 15 V Bias for Red A. 28
Figure 24. Current as a Function of Time Following Application of 15 V Bias for Red B. 29
Figure 25. Current as a Function of Time Following Application of 15 V Bias for Yellow B 30
Figure 26. Transient Current of Red A at 6°C Following Application of 15 V Bias. 31
Figure 27. Current and Light Output as a Function of Time Following Application of 15 V Bias for Red A. 32
Figure 28. Current and Light Output as a Function of Time Following Application of 15 V Bias for Red B. 33
Figure 29. Current and Light Output as a Function of Time Following Application of 15 V Bias for Yellow B. 34
Figure 30. Capacitance as a Function of Time Following Application of 15 V Bias for Red A. 35
Figure 31. Capacitance as a Function of Time Following Application of 15 V Bias for Red B. 36
Figure 32. Capacitance as a Function of Time Following Application of 15 V Bias for Yellow A. 37
Figure 33. EC Model of P-N Junction Formation [From 6]. 38

Figure 34. Activation Energy (*E*) of Ion Hopping in PEO. 39
Figure 35. Arrhenius Plot of Rate of Change of Capacitance as a Function of Inverse Temperature for Yellow A. 40
Figure 36. Normalized Change in C, L and I as a Function of Time for Red A at 10°C. 41
Figure 37. Normalized Change in C, L and I as a Function of Time for Red B at 10°C. 42
Figure 38. Normalized Change in C, L and I as a Function of Time for Yellow A at 2°C. 43
Figure 39. Current as a Function of Time Following Application of Different Bias Voltage for Yellow 6b. T = 15°C. 46
Figure 40. Current as a Function of Time Following Application of Different Bias Voltage for Yellow 5b. T = 15°C. 47
Figure 41. Light Output as a Function of Time Following Application of Different Bias Voltage for Yellow 6b. T = 15°C. 48
Figure 42. Light Output as a Function of Time Following Application of Different Bias Voltage for Yellow 5b. T = 15°C. 49
Figure 43. Capacitance as a Function of Time Following Application of Different Bias Voltage for Yellow 6b. T = 15°C. 50
Figure 44. Capacitance as a Function of Time Following Application of Different Bias Voltage for Yellow 5b. T = 15°C. 51
Figure 45. Final Capacitance Value as a Function of Bias Voltage for Yellow 6b. 52
Figure 46. Final Capacitance Value as a Function of Bias Voltage for Yellow 5b. 53
Figure 47. Normalized Change in C, L and I as a Function of Time for Yellow 6b at 8 V. 54
Figure 48. Normalized Change in C, L and I as a Function of Time for Yellow 5b at 8 V. 55
Figure 49. Normalized Change in C and I as a Function of Time for Yellow 5b at 6 V. 56
Figure 50. Capacitance as a Function of Time Following Application of Different Bias Voltage for Yellow 5b at 22°C. 57
Figure 51. Normalized Change in C, L and I as a Function of Time for Yellow 5b with 5 V at 22°C. 58
Figure 52. Normalized Change in C, L and I as a Function of Time for Yellow 5b with 4 V at 22°C. 59

LIST OF ACRONYMS AND ABBREVIATIONS

A/D	Analog to Digital
Al	Aluminum
Ag	Silver
AVI	Add-Vision, Inc.
C	Capacitance
DAQ	Data Acquisition Board
EC	Electrochemical
ED	Electrodynamic
GPIB	General Purpose Interface Bus
I	Current
IFF	Identification Friend or Foe
IR	Infrared
ITO	Indium Tin Oxide
LEC	Light-Emitting Electrochemical Cell
Li Triflate	Lithium Trifluoromethanesulfonate
NVG	Night Vision Goggles
OIF	Operation Iraqi Freedom
OLED	Organic Light Emitting Diode
Opamp	Operational Amplifier
OSD	Office of Secretary of Defense
PEO	Polyethylene Oxide
P-OLED	Polymer Organic Light Emitting Diode
PPV	Poly(p-phenylene vinylene)

R	Resistance
TTI	OSD Technology Transition Initiative
Z	Impedance
Z_I	Imaginary Impedance
Z_R	Real Impedance

ACKNOWLEDGMENTS

This work was supported in part by the Technology Transition Initiative of the Office of the Director of Defense Research and Engineering (DDRE) and in part by the National Science Foundation under grant DMR 0804527.

I would like to thank Sam Barone and George Jaksha for their assistance and skills on the material side of getting my experiments up and running.

Thank you to Dr. Devin Mackenzie and his staff at Add-Vision Inc. for the all IIFF patch samples and the information provided to help me further understand this work.

Thank you to my small group of classmates who endlessly pointed out my flaws but always provided the support when it was needed. I couldn't have picked a better group of guys to have spent the last eight quarters sitting next to.

Thank you to Dr. Nancy Haegel whom I admired as a woman and physicist since the first day I met her. You are a true inspiration and I will always appreciate your dedication to my journey in search of higher learning and the constant need for "one more experiment!"

To Dr. Peter Crooker I must give the most thanks. Thank you for your idea, which led to this research. Thank you for your invaluable though "ugly" LabView programming, which allowed me to collect more data than anyone will ever be able to fully appreciate. Thank you for your attention to detail and eagerness to teach. Most of all, I thank you for your time and patience as the last two years of my life could not have possibly been better spent under the tutelage of any other. You could never be the lowest hanging fruit in my department.

A very special thank you to my mother, father and sisters for always answering the phone, not matter the time of day, and listening to me whine about the trials and tribulations of physics. I would not be where I am today without your love, understanding and continued support of all my choices. And finally, I would like to thank Alfredo for loving me and appreciating just how smart I really am.

THIS PAGE INTENTIONALLY LEFT BLANK

I. INTRODUCTION

A. MOTIVATION FOR DEVICE USE

Fratricide, defined as the killing of one's own countryman, has always been a problem in combat. During Operation Iraqi Freedom (OIF), in only March through April of 2003, 45% of U.S. deaths were due to fratricide [1]. In an effort to reduce fratricide in today's complex battlefield environment, new and emerging technologies have been leveraged to produce individual identification patches for soldiers. One type of patch prominent on the battlefield today is an infrared (IR) reflective patch produced to look like a U.S. flag that soldiers velcro on the shoulder of their uniforms, as seen in Figure 1. These devices provide a directionally dependent reflection of any IR source, such as a laser or very bright flashlight.

Figure 1. IR Reflective Patch.

However, this IR reflective patch is not covert due to the abundance of night vision goggles (NVGs) in both friendly and enemy hands today. There will be a reflection of any IR illumination of the soldier, which will be visible by an IR-equipped observer. To help reduce fratricide numbers, there is a need for a low-cost covert ability to identify soldiers as friend or foe that is easily integrated into existing operational procedures. In 2009, the Office of the Secretary of Defense (OSD) directed the

Technology Transition Initiative (TTI) program to fund the Polymer Light Emitting Diode (P-OLED) Enabled Individual Identification Friend or Foe (IFF) project [2].

The goal of this project was to produce a small flexible device, to be used in a patch similar to Figure 1, that responds by emitting IR light only when interrogated by a U.S. targeting laser. A device like this would be covert because it will respond only to specific signals used exclusively by friendly forces. The Light-Emitting Electrochemical Cell (LEC) described in this work was manufactured by Add-Vision, Inc., (AVI) in support of this project. The LEC is an excellent option for this use because it is small, light and flexible. Its emission spectra can be tuned for the IR wavelengths, and it has both low cost and ease of manufacturing compared to other types of Organic Light Emitting Diodes (OLEDs).

The device is operated by applying a voltage across an organic polymer, causing the polymer to emit light. This mode of operation is similar to that of the more common OLED; however, the LEC is unique because it consists of organic polymers and the behavior is electro-chemical. Ordinary OLEDs are solid-state devices with built-in junctions, while the LEC junction is dynamic. Device operation will be discussed in Chapter II.

B. MOTIVATION TO STUDY DEVICE

Outside of this specific military application, the LEC is also an attractive option for a wide range of display and signaling technologies. Despite its many possible uses and ease of manufacturing, the underlying physics of the device's mode of operation—specifically the dynamic junction formation—is still not fully understood.

Since the patent for the LEC in 1994 [3], several studies have been performed in an effort to understand and model the mechanisms responsible for the LEC's behavior. Two models, the Electrochemical (EC) and Electrodynamic (ED), have emerged with data supporting both viewpoints. In response to questions arising from these studies the IFF LEC patch will be used to make measurements of the device's capacitance, resistance, current and light output as functions of temperature and voltage to further

understand both the fundamental physics and the limitations of variable temperature application. All previous published work to measure capacitance has been performed statically. The work presented here is a continuation of work performed at NPS by LT Karl Burnett [4]. This thesis will add dynamic capacitance measurements to Burnett's previous studies of transient current and light output. This work will be the first to concentrate specifically on the transient capacitance of LECs.

C. THESIS OVERVIEW

The goal of this work is to make the first transient capacitance measurements of an LEC. This information, along with the transient current and light output will be characterized. Chapter I describes the motivation behind this research. Chapter II presents LEC structure and the theories of operation behind the EC and ED models. Chapter III describes the experimental setup and data collection process. In Chapter IV, the temperature dependent measurements and data are presented and discussed. In Chapter V, the voltage dependent measurements and data are presented and discussed. Chapter VI presents conclusions and suggestions for future work.

THIS PAGE INTENTIONALLY LEFT BLANK

II. THEORIES OF OPERATION

A. CONSTRUCTION AND COMPOSITION OF LECS

The acronym LEC actually leaves out one very important defining part of all LECs—the P for polymer. A light-emitting polymer is the essential component. A typical LEC consist of a layer of light-emitting polymer between two electrodes. Common electrodes are indium tin oxide (ITO), aluminum (Al), and silver (Ag). Most research LECs discussed in the literature are *planar* devices like that shown in Figure 2. The AVI LEC uses a silver cathode and a transparent ITO anode in a *sandwich* device as illustrated in Figure 3.

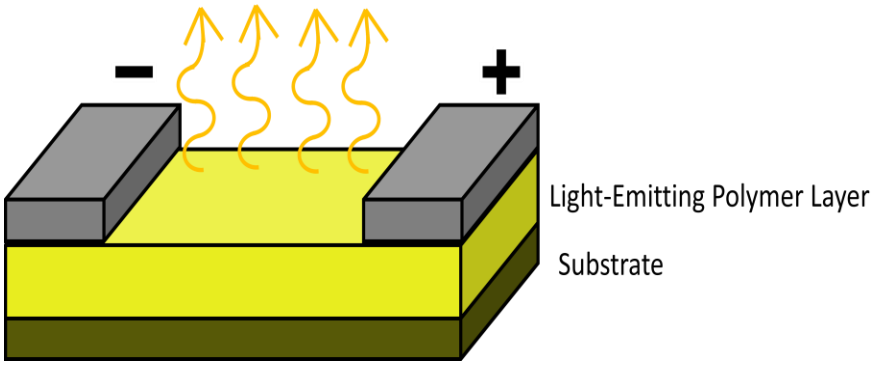

Figure 2. Planar LEC.

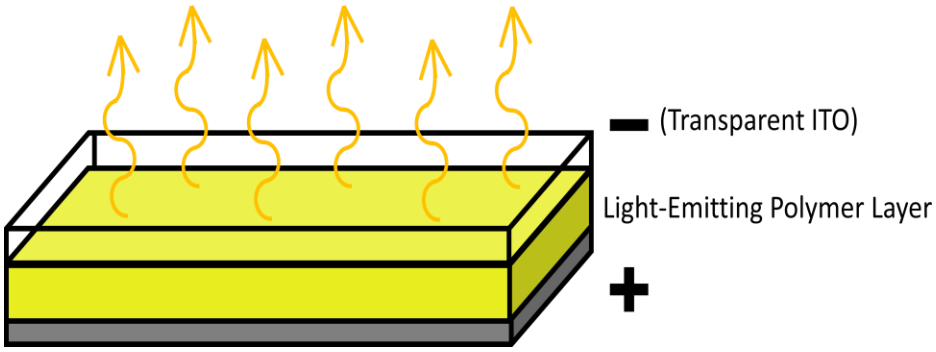

Figure 3. Sandwich LEC.

LECs usually consist of a blend of two polymers and a salt. One polymer conducts electrons and holes and is luminescent, while the other enhances transport of the salt ions. A common light-emitting polymer is poly(p-phenylene vinylene) or PPV. Figure 4 shows the chemical structure of PPV.

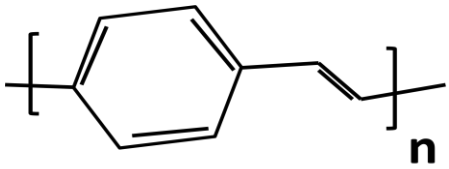

Figure 4. Chemical Structure of PPV.

An example of an ionic conducting polymer is poly(ethylene oxide) or PEO. Together with the salt lithium trifluoromethanesulfonate (Li triflate), they form a common polymer electrolyte that is ionically conductive. Figure 5 shows the chemical structure of PEO.

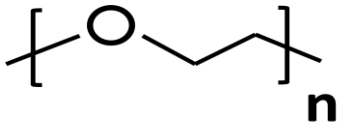

Figure 5. Chemical Structure of PEO.

Although the two polymers are blended together in one layer, they are not dissolved within one another as a solid solution. It is convenient to think of the PPV and PEO as separate highways that never intersect, though they do pass over and under one another. The electrons and holes travel only on the PPV highway, while the ions travel only on the PEO highway.

B. GENERAL MODE OF OPERATION

The following steps are common to all models of the LEC [5]. A bias voltage applied across the electrodes creates an electric field within the polymer layer. The salt ions migrate towards their oppositely charged electrodes: negative anions toward the positive anode; positive cations toward the negative cathode. Electrons and holes are injected and recombine somewhere within the polymer layer and light is emitted. The relative rates and importance of the electron, hole and ion motion on their respective highways and the resulting electric field distribution are the issues that are debated between the EC and ED models.

C. THE ELECTROCHEMICAL MODEL

The EC model was first proposed by Heeger *et al.* in 1995 [5], the same group responsible for the 1994 LEC patent. They state that light emission is due to a p-n junction that is formed within the polymer layer. A detailed description of what is happening on the anode side and cathode side of the polymer layer illuminates how the p-n junction is formed and is illustrated in Figure 6 [6].

1. Anode

Positive voltage is applied at the anode. An electron is removed from (i.e., a hole is injected into) the PPV. The removed electron oxidizes the PPV, which is now positively charged and possesses a mobile hole. A negative salt anion then moves into the same region via the PEO and restores the local charge balance. This region is now neutral but contains a mobile hole—making it p-type. This is analogous to a p-type semiconductor with negative ionized acceptor sites, such as an ionized boron site [B-] in silicon [Si] and its associated hole in the valence band.

2. Cathode

Negative voltage is applied at the cathode. An electron is injected into the PPV. The injected electron reduces the PPV, which is now negatively charged and possesses a mobile electron. A positive salt cation then moves into the same region via the PEO and restores the local charge balance. This region is now neutral but contains a mobile electron – making it n-type. This is analogous to an n-type semiconductor with positively charged donor impurities, such as an ionized phosphorus site [P+] in Si and its associated free electron in the conduction band. Thus, in this model, the doping and junction formation occurs with the application of bias. In this respect, the LEC is very different than a conventional inorganic semiconductor.

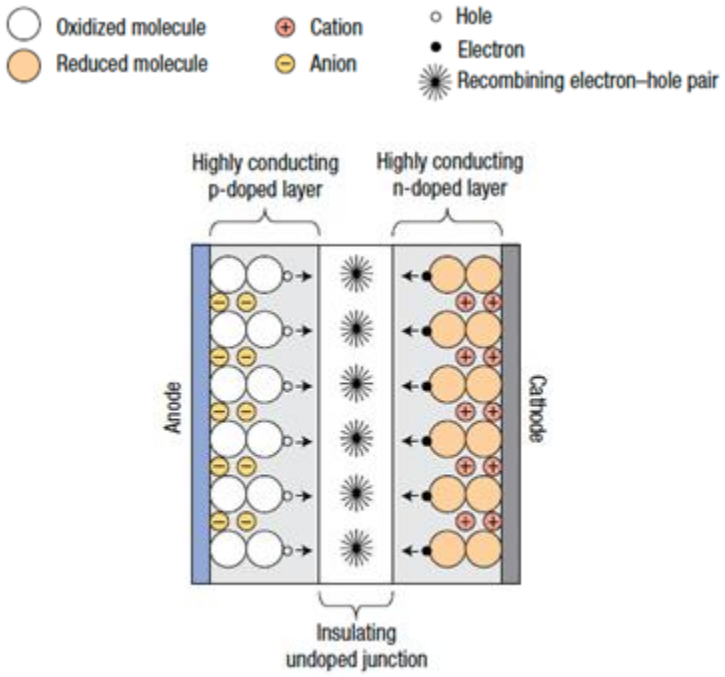

Figure 6. Electrochemical (EC) Model of P-N Junction Formation [From 6].

The formation of a p-n junction within the polymer layer leads to an explanation of how the electric field under bias is changing across the layer as well. The p-type and n-type regions are electrically conducting so the electric field in these regions is zero. The recombination zone is where the majority of the electric field exists as depicted in Figure 7.

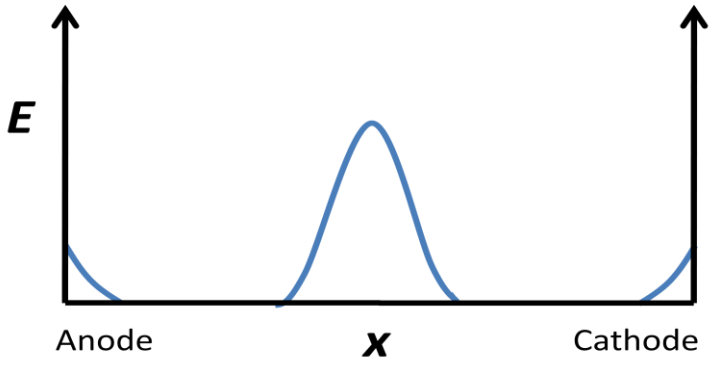

Figure 7. Electric Field in EC Model.

Data and theory supporting the EC model were published by Pei *et al.* [7], Dick *et al.* [8], Smith [9] and Campbell *et al.* [10] from 1996 through 1998. Among other results, Pei [7] presented current-light-voltage characteristics of an LEC as shown in Figure 8. Smith presented a steady state model [9], which he followed up with a presentation of capacitance measurements in conjunction with Campbell [10], as shown in Figure 9.

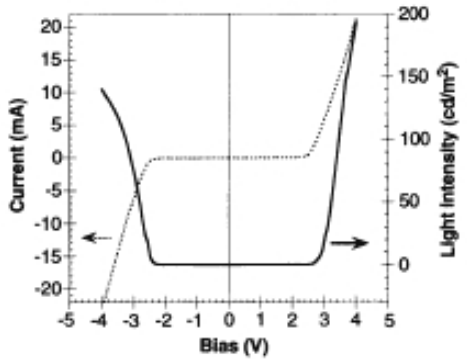

Figure 8. Current-Light-Voltage Characteristics [From 7].

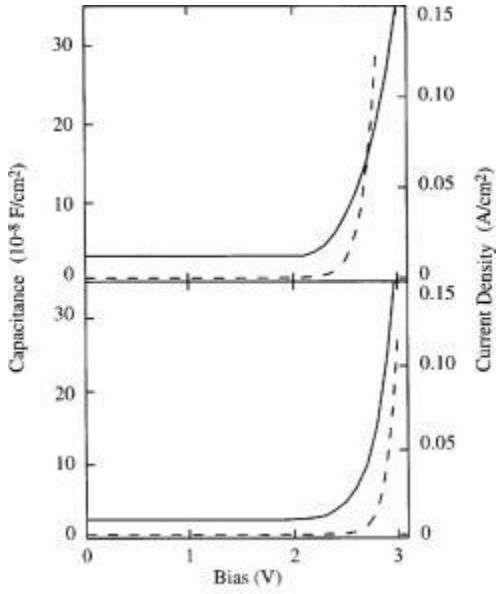

Figure 9. Capacitance-Voltage and Current-Voltage Characteristics [From 10].

D. THE ELECTRODYNAMIC MODEL

The ED model was first proposed by deMello *et al.* in 1998 [11]. They suggest that light emission is due to diffusion of charge carriers within the polymer layer. Again, a detailed description of both the anode and cathode side will illustrate the phenomena shown schematically in Figure 10 [6].

1. Anode

Positive voltage is applied at the anode. Negative anions migrate toward the anode and an excess of anions accumulates at the anode. The interface region now has a double charge layer and the resulting high electric field at the interface increases hole injection by enabling tunneling through the contact barrier. The mobile hole then diffuses into the now neutral bulk of the polymer layer.

2. Cathode

Negative voltage is applied at the cathode. Positive cations migrate toward the cathode and an excess of cations accumulates at the cathode. The interface region now has a double charge layer and the resulting high electric field at the interface increases electron injection by enabling tunneling through the contact barrier. The mobile electron then diffuses into the now neutral bulk of the polymer layer.

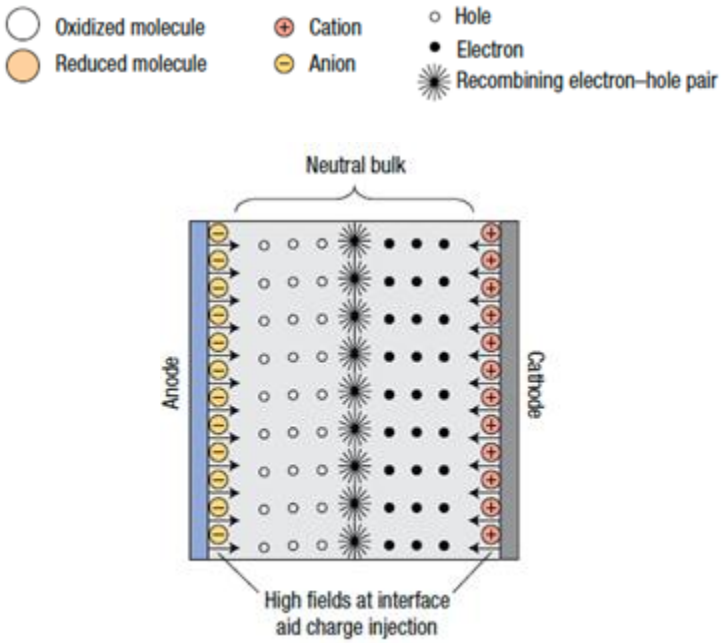

Figure 10. Electrodynamic (ED) Model of Charge Diffusion [From 6].

The diffusion of charge carriers into the neutral bulk of the polymer layer also leads to an explanation of how the electric field is changing across the layer. The electric field only exists near the electrodes, while in the recombination zone the electric field is nearly zero as depicted in Figure 11.

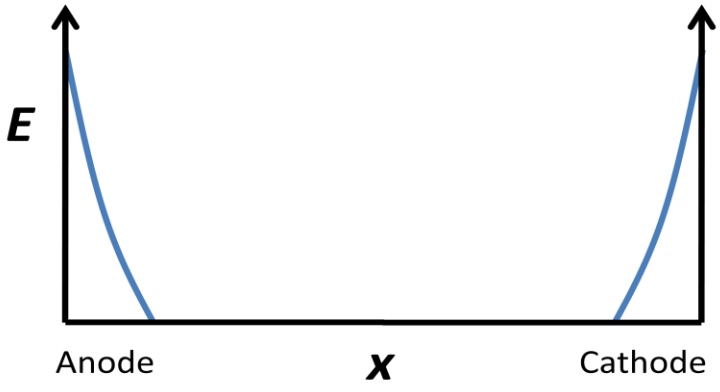

Figure 11. Electric Field in ED Model.

Data and theory supporting the ED model were published by deMello *et al.* [11], Slinker *et al.* [12], and Pingree *et al.* [13] as early as 1998 and through 2007. Slinker used electric field microscopy to map the potential and electric field of an LEC, shown in Figure 12, while Pingree used scanning Kelvin probe imaging to map the potential, field and charge of planar LECs. Both observed evidence for large field variations primarily near the contacts.

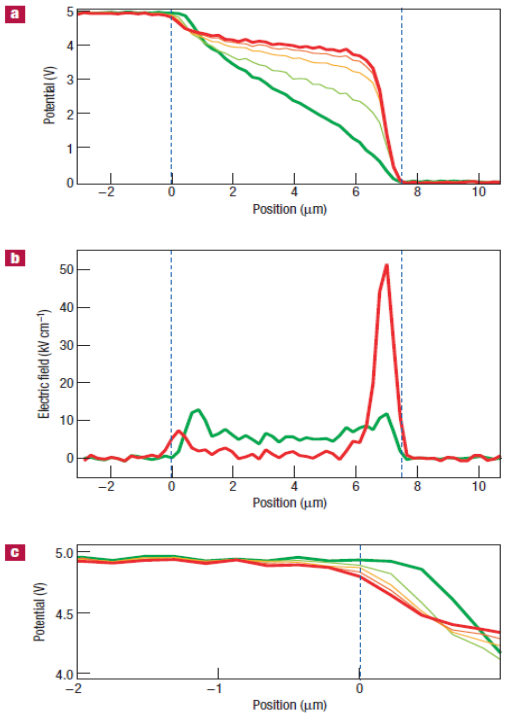

Figure 12. Mapping of Potential and Electric Field of LEC [From 13].

E. A UNIFYING MODEL

In 2010, Edman [14] presented a unifying model that incorporated both models as limits. He addressed both models, paying particular attention to how the contacts affect the dynamic junction behavior. In a previous publication, Edman [15] had used the EC model to present his data, but in his 2010 publication he suggests that an LEC will follow

one model or the other depending on the injection rate at the contacts of the LEC. He presents simulation data and refers to the EC model as Non-injection limited and the ED model as Injection limited.

F. APPLYING THE MODELS

Both the EC and ED models present plausible theories of operation with some supporting data. The question remains whether either model, or some hybrid theory is correct. It is not our goal to prove or disprove either theory. We collect data on the transient capacitance, current and light emission and then analyze and compare each in effort to reach a better understanding of ion motion inside the LEC. However, the models will be used to further our understanding and provide insight into the experimental results. Specifically, we will attempt to describe how the junction forms in the IFF LEC, much like what is done in both model theories, with particular attention to the mechanisms that affect the transient capacitance behavior.

III. EXPERIMENTAL SETUP AND DATA COLLECTION PROCESS

A. GENERAL EXPERIMENTAL SETUP

Every experiment and data collection process was run in a similar manner. An LEC was connected to a power source, placed in a stand next to a photodiode and the stand was placed inside the temperature chamber. All devices were placed in the chamber for one hour, at temperature, prior to commencing any run in order to ensure the LEC came to the specified temperature. All other equipment was turned on and electrical connections were checked. If the experiment was conducted with a constant voltage source, the Agilent 4294A Precision Impedance Analyzer was used to provide the voltage bias. If the experiment was designed for a constant current source, the Keithley 220 Programmable Current Source was used to provide the current. The LEC identification number (ID#), date and temperature were recorded. Experimental parameters were input into a LabView 8.6 program called OLED3, which is detailed later in this chapter. The source was turned on and data were collected for the specified time period. A schematic of the setup with the Agilent as the source is shown in Figure 13.

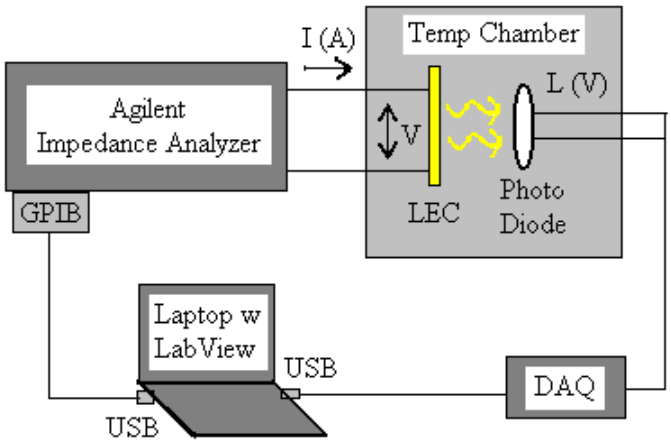

Figure 13. General Experimental Setup.

B. ELECTRICAL CONNECTIONS OF THE IFF LEC

Several LEC devices are pictured in Figure 14. As can be seen in Figure 14, each LEC device actually has two emitter cells with their own electrical connections. An LEC was connected to a source through a daughter board, supplied by AVI, as pictured in Figure 15.

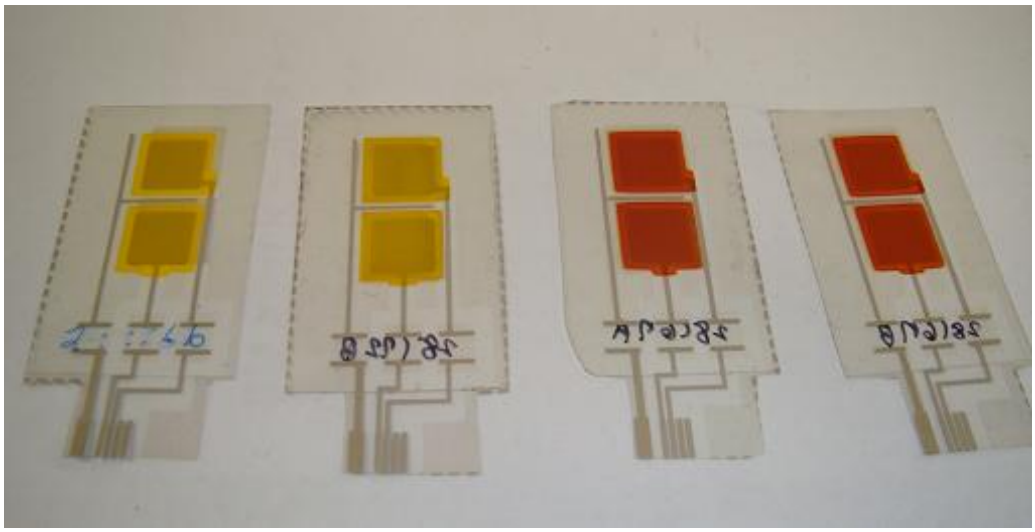

Figure 14. LEC Devices.

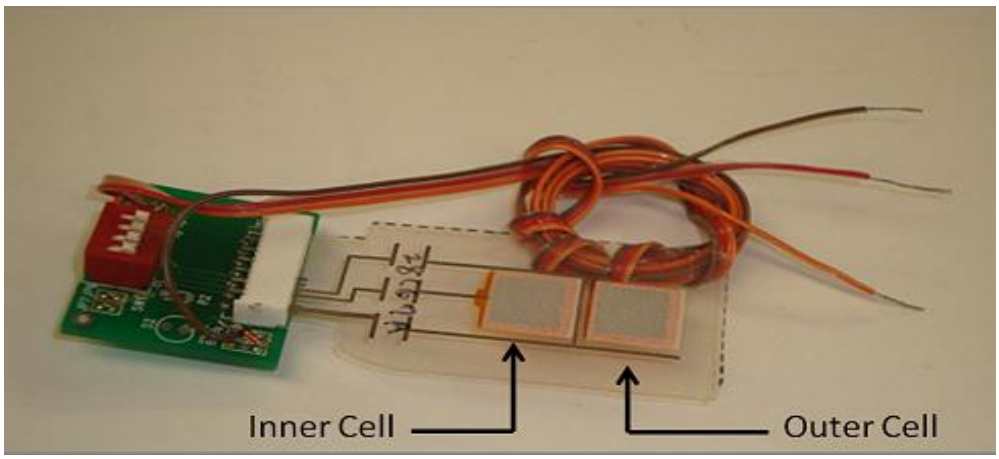

Figure 15. LEC Connected to Daughter Board.

The daughter board was connected to the project board via a tri-wire where the brown wire is the common ground, the red wire is the source for the inner cell and the orange wire is the source for the outer cell. The two cells within the LEC can be independently or cooperatively activated. Only one cell was activated at a time, therefore, only the orange or red wire was attached, for all experiments. The daughter board was wired to the source on a project board via a double-pole, double-throw switch. The switch allowed for a simple mechanical switch between the current or voltage source without having to rewire the project board. The schematic is pictured in Figure 16.

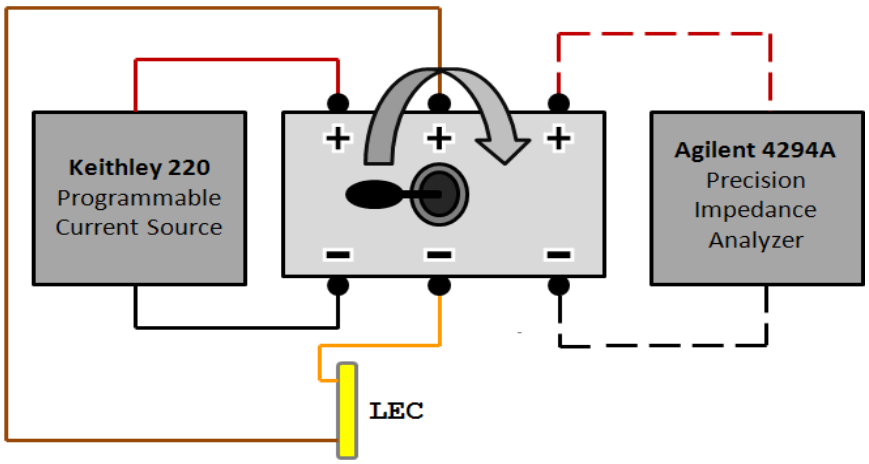

Figure 16. Schematic of LEC and Switch Wiring.

C. COLLECTION OF LIGHT OUTPUT

A photodiode was used to measure the light output of the LEC. The photodiode was placed approximately 3 cm from the LEC surface and centered on the cell that was being activated. An operational amplifier (opamp), with a 5.1 MΩ resistor and 3.3 nF capacitor in parallel, was used to convert the photocurrent (I) to voltage, as shown in Figure 17.

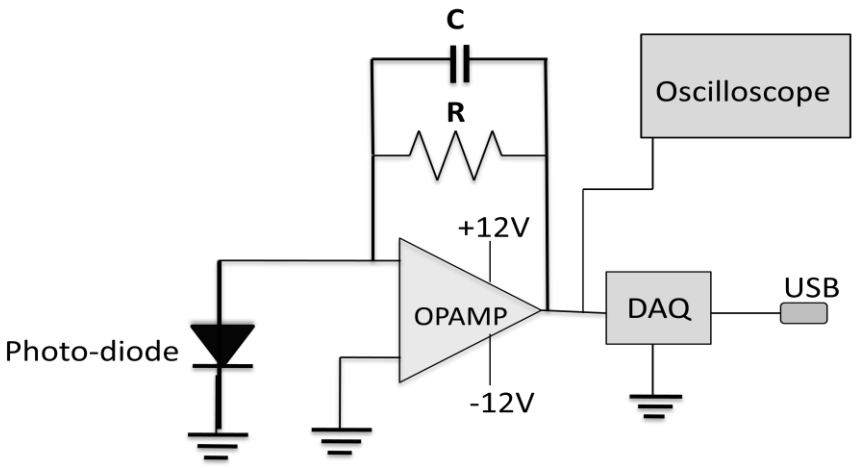

Figure 17. Schematic of Photodiode and DAQ Setup.

The intensity of optical emission from the LEC is proportional to the photocurrent and hence to the resulting DC voltage:

$$Light \propto I \ = \frac{V}{Z} = \frac{V}{R//C} \tag{1}$$

$$V = \frac{IR}{1 + j\left(\frac{f}{f_C}\right)} = DC\ voltage \propto Light \text{ Intensity.} \tag{2}$$

The capacitor rolls off frequencies higher than 9.5 Hz in order to decrease the noise in the collected data per Equation 3, depicted in Figure 18. This was acceptable because we took one measurement per second, a sample rate of 1 Hz.

$$f_C = \frac{1}{2\pi RC} = \frac{1}{2\pi(5.1M\Omega)(3.3nF)} = 9.5\ Hz \tag{3}$$

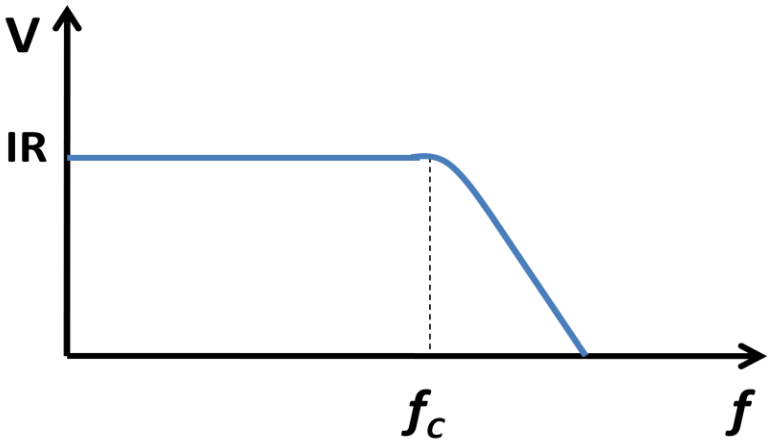

Figure 18. Cutoff Frequency Due to Capacitor.

The DC voltage was then read by a National Instruments Data Acquisition Board (DAQ model USB-6211) which uses a 16-bit analog to digital (A/D) converter. The DAQ received input parameters via USB connection to a laptop running the OLED3 program. Input parameters for the DAQ include samples/s, voltage range, number of samples and timeout, which can be seen on the Front Panel of OLED3 in Figure 22.

OLED3 received the light output data as a string and saved the data as a text file after completing each experiment. Since the device and photodiode were inside the temperature chamber and could not be visually observed, an oscilloscope was connected to the photodiode voltage to monitor light output in real time (Figure 17).

D. TEMPERATURE CHAMBER

The temperature chamber used for all experiments was a Tenney Junior Environmental Test Chamber Model TJR, pictured in Figure 19.

Figure 19. Temperature Chamber.

Placing the LEC and photo-diode inside the temperature chamber ensured there was no ambient light during the experiment. The temperature chamber was operated in Celsius mode and controlled via the digital panel user interface which allowed a precision of 0.1°C.

E. CURRENT SOURCE

A constant current was supplied by the Keithley 220 Programmable Current Source. The current source was manually set up in a continuous program mode. The compliance voltage was always set at 30 V while the current was selected based on experimental requirements.

F. VOLTAGE SOURCE

A DC bias voltage was supplied by the Agilent 4294A Precision Impedance Analyzer. The Agilent was operated in the R-X mode which measures the real (Z_R) and imaginary (Z_I) parts of the impedance (Z). In order to reduce the amount of time required

to interrogate the LEC, five frequencies were selected; 40 Hz, 283 Hz, 2 kHz, 14.1 kHz and 100 kHz. In the R-X mode the Agilent interrogates the LEC over the five frequencies and displays Z_R vs. frequency (top window) and Z_I vs. frequency (bottom window) on its front panel as shown in Figure 20.

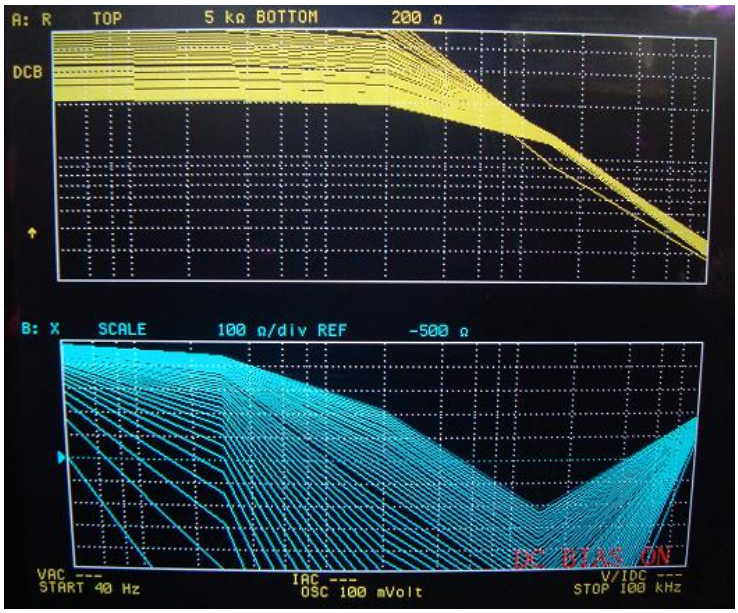

Figure 20. Display of Agilent in R-X Mode.

The impedance analyzer is connected to a laptop running OLED3 via a General Purpose Interface Bus (GPIB). The OLED3 program sends input parameters to the Agilent and receives the output impedance data. Input parameters for the Agilent include the run duration in seconds, samples/s, bias voltage, number of frequencies to interrogate, and the current limit. These parameters can be seen on the Front Panel of OLED3 in Figure 22.

The impedance analyzer applies the specified bias voltage to the LEC and then modulates this voltage at the specified frequencies. By modulating the voltage the impedance analyzer interrogates the LEC in order to measure the real and imaginary parts of the LEC's impedance.

G. LABVIEW 8.6 PROGRAM OLED3

The LabView 8.6 program OLED3 was the key control of every experiment. It was responsible for not only sending input parameters to and receiving data from both the Agilent and DAQ, but also calculating the transient resistance (R), capacitance (C) and current (I). OLED3 displays the instantaneous current in real time and upon the completion of each experiment I, R and C are displayed in graphical form on the Front Panel, Figure 22. All of this data is saved in matrix form to a text file on the laptop. Light output data from the DAQ is also displayed graphically and saved in matrix form as a separate text file.

1. Model of the LEC

In order to calculate I, R and C of the LEC we modeled it as a capacitor and resistor in parallel as shown in Figure 21.

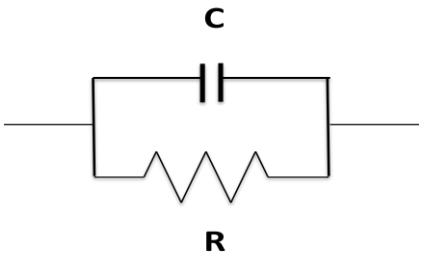

Figure 21. LEC Electrical Model as Resistor and Capacitor in Parallel.

In addition, there is also a small resistance r in series with R//C due to the contacts at the electrodes of the LEC. We ignore r in the following calculation because it only affects the results at high frequencies where R~r. All data were analyzed at the lowest frequency of 40 Hz.

2. Calculating R, C and I

The impedance analyzer receives the input parameters from OLED3 and returns the real (Z_R) and imaginary (Z_I) part of the LEC's impedance (Z) per Equation 4, where $j^2 = -1$.

$$Z = Z_R - jZ_I \tag{4}$$

Since the LEC is modeled as a capacitor and resistor in parallel Equations 5 and 6 follow.

$$\frac{1}{Z} = \frac{1}{R} + \frac{1}{(1/\ j\omega C)} \tag{5}$$

$$Z = \frac{1}{1 + j\left(\frac{\omega}{\omega_0}\right)} = \frac{R}{1 + \left(\frac{\omega^2}{\omega_0^2}\right)} - j\frac{R\left(\frac{\omega}{\omega_0}\right)}{1 + \left(\frac{\omega^2}{\omega_0^2}\right)} \tag{6}$$

With $\omega_0 = 1/RC$, we find Z_R and Z_I in Equations 7 and 8 respectively.

$$Z_R = \frac{R}{1 + \left(\frac{\omega^2}{\omega_0^2}\right)} \tag{7}$$

$$Z_I = R\frac{\left(\frac{\omega}{\omega_0}\right)}{1 + \left(\frac{\omega^2}{\omega_0^2}\right)} \tag{8}$$

A fit of the data to the model of (7) and (8) allowed the extraction of R and C at various frequencies. The end results are Equations 9 and 10 for R and C.

$$R(f) = Z_R + \frac{Z_I^2}{Z_R} \tag{9}$$

$$C(f) = \frac{Z_I}{2\pi f \left| Z_R^2 + Z_I^2 \right|} \tag{10}$$

OLED3 calculates I with the input parameter of the bias voltage and the calculated R from (9) at the lowest frequency per Equation 11.

$$I = \frac{V_B}{R} \tag{11}$$

Finally, OLED3 performs all of these calculations and stores the data in a large matrix. The programming for OLED3 can be seen on the Block Diagram of the OLED3 LabView program in the attached supplemental. An electronic version can be accessed by clicking here, or by referencing the insert attached to the printed version of this thesis.

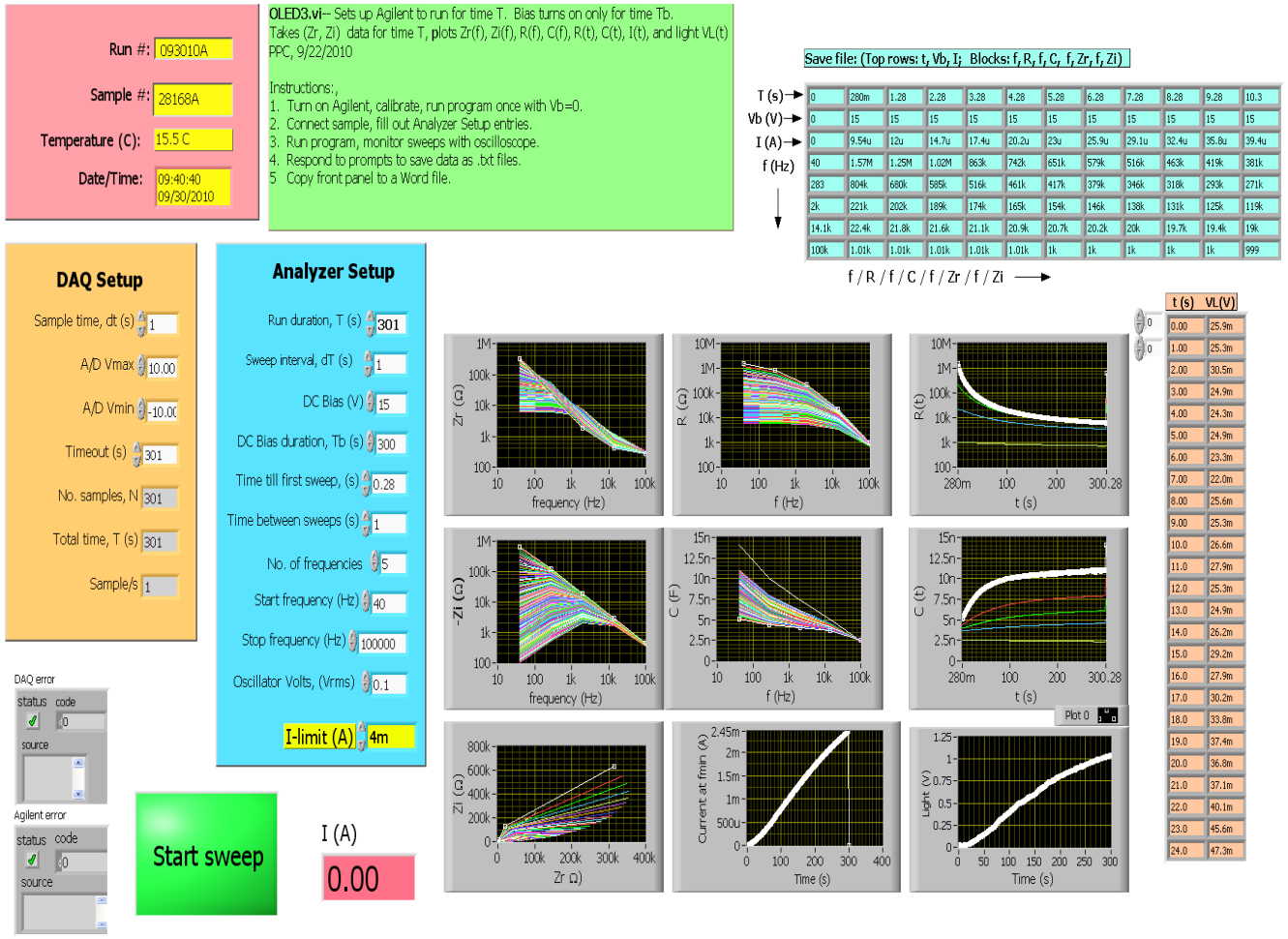

Figure 22. OLED3 Front Panel

THIS PAGE INTENTIONALLY LEFT BLANK

IV. TEMPERATURE DEPENDENT MEASUREMENTS

A. LEC TURN-ON TRANSIENTS

The LEC devices manufactured by AVI for this project underwent several generations of development. First-generation devices exhibited a very slow initial turn-on time and AVI minimized this transient behavior in second- and third-generation devices with different polymer modifications. All LECs used in the following experiments were third-generation devices. Three different LECs were used; two devices designed for enhanced emission in the IR, ID#28168A (Red A) and ID#28167B (Red B), and one device that emitted primarily in the visible yellow, ID#28172B (Yellow B).

Our goal was to measure transient current, light output and capacitance specifically targeting the turn-on time period for the devices. In order to capture these measurements over varying turn-on times, we conducted the same experiment over a range of temperatures. During every experiment, the bias voltage was 15 V. Previous work by Burnett [4] and our own initial experiments run on test devices provided valuable knowledge about device survivability. Consequently, a maximum current of 4 mA was imposed in order to avoid device damage. After completing experiments on Red A, the OLED3 program was modified to turn off the bias voltage if the current exceeded 4 mA.

B. TEMERATURE DEPENDENCE OF CURRENT

Work by Burnett demonstrated that current increased during the turn-on time when the LEC was under constant bias voltage. Burnett's temperature range was between -16°C and 4°C, while our temperature range was between 4°C and 26°C. As expected, we observed the same general behavior. We also observed that as temperature decreased the *rate* of current increase also decreased, i.e., the slope of current vs. time decreased. The same behavior was observed in all three LECs and is shown in Figures 23, 24 and 25.

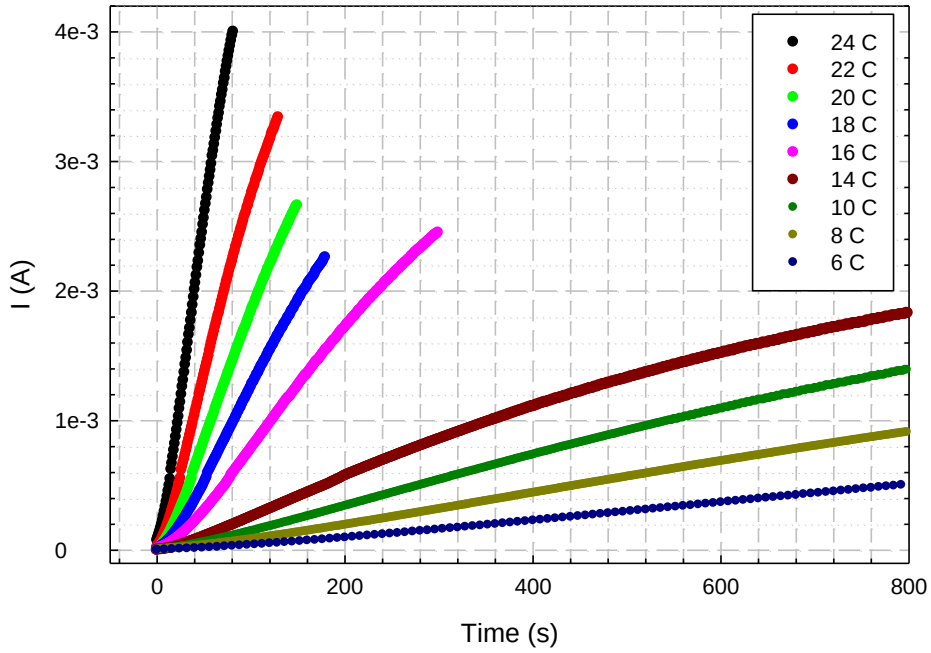

Figure 23. Current as a Function of Time Following Application of 15 V Bias for Red A.

It is important to notice the time scale in each of Figures 23-25. Red A takes approximately 40 seconds to reach 4 mA at 24^{0}C, while Red B takes approximately 12 seconds and Yellow B only 4 seconds at the same temperature. Yellow B consists of the same material that AVI uses for its commercial products—it does not contain the additives put in the red devices that cause them to emit in the IR. The lack of these additives accounts for the shorter turn-on time observed in Yellow B.

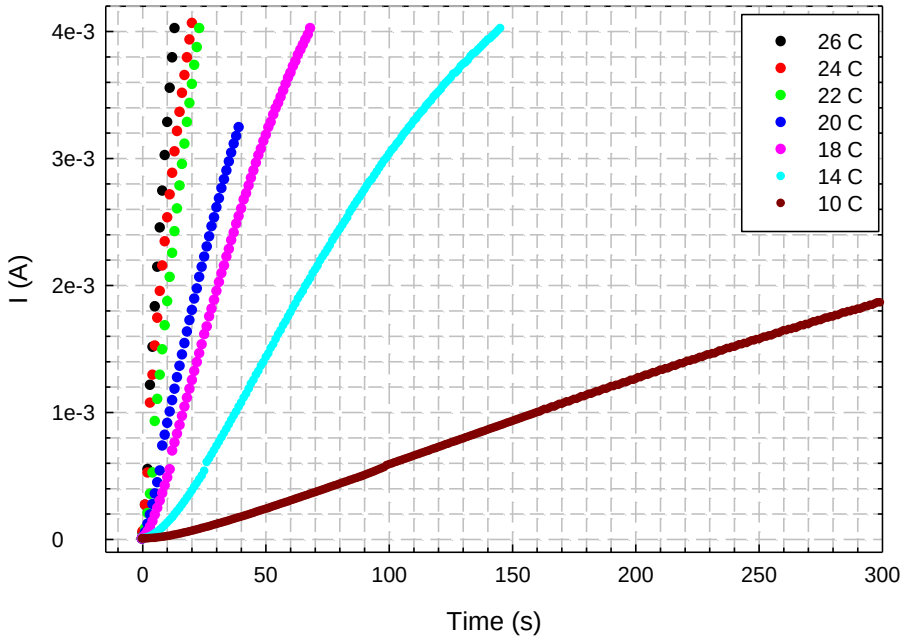

Figure 24. Current as a Function of Time Following Application of 15 V Bias for Red B.

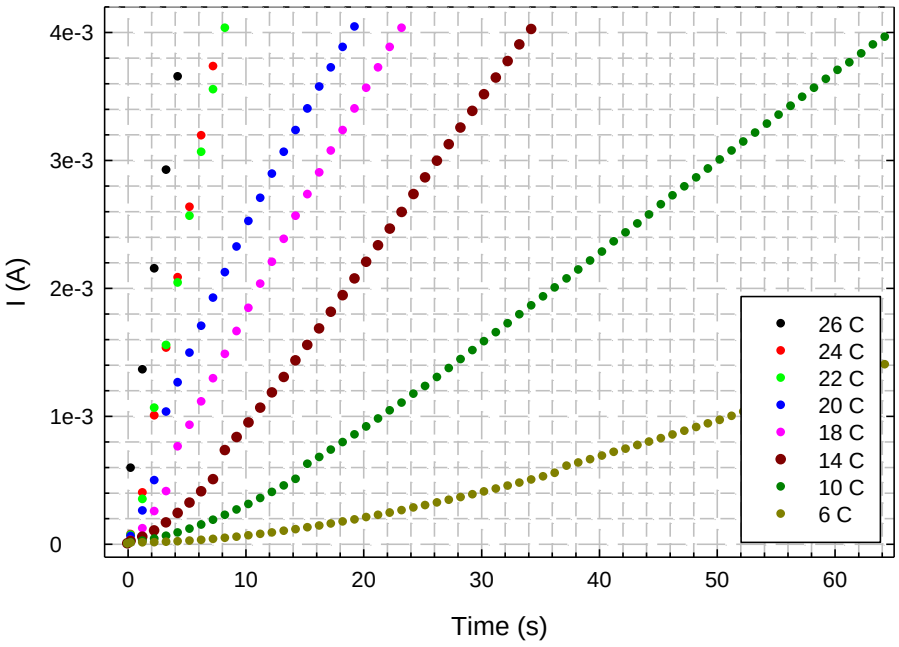

Figure 25. Current as a Function of Time Following Application of 15 V Bias for Yellow B

Higher temperatures caused a significant change in the initial rate of change of the current. Ion motion is very temperature dependent and this temperature dependent current behavior supports ion motion playing a major role in the transient current response.

By examining the 6°C run for Red A, Figure 26, we analyze another interesting phenomenon observed in all three LECs. There is an initial, steeper slope in current and then around the 2200 second mark the slope decreases. We hypothesize that the initial, steeper slope is due to ion motion contributing to current in two ways; 1) ions accumulating near the electrodes lower the contact barriers and enhance free carrier injection, contributing to the classic drift current, and 2) ion motion within the LEC contributes to the displacement current (dE/dt) because their motion causes the E field to change in time after the application of bias voltage. The smaller slope at longer times is

associated with changes in traditional drift current, which we believe would eventually level out because the E field would stop changing in time and reach a steady state.

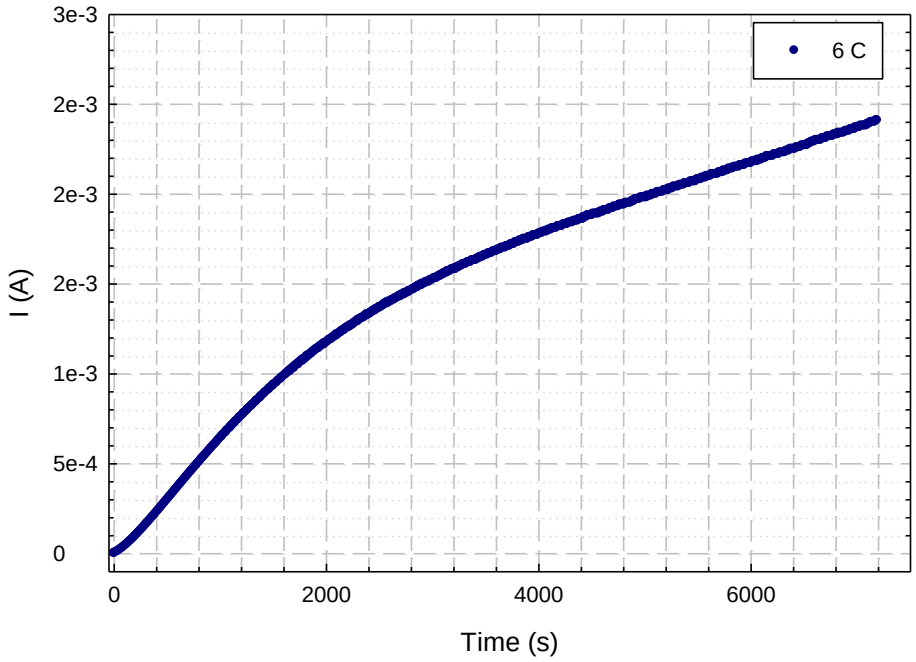

Figure 26. Transient Current of Red A at 6°C Following Application of 15 V Bias.

C. CORRELATION BETWEEN CURRENT AND LIGHT OUTPUT

There is a direct correlation between current density and light output: as current density increased the light output also increased. This can be clearly seen by plotting the total current and light output for each LEC on the same graph, shown in Figures 27, 28 and 29. The following three graphs are plotted with logarithmic axes in order to accommodate the wide range of time scale on the x-axis and the difference in vertical scale for light output and current, which are both plotted on the y-axis.

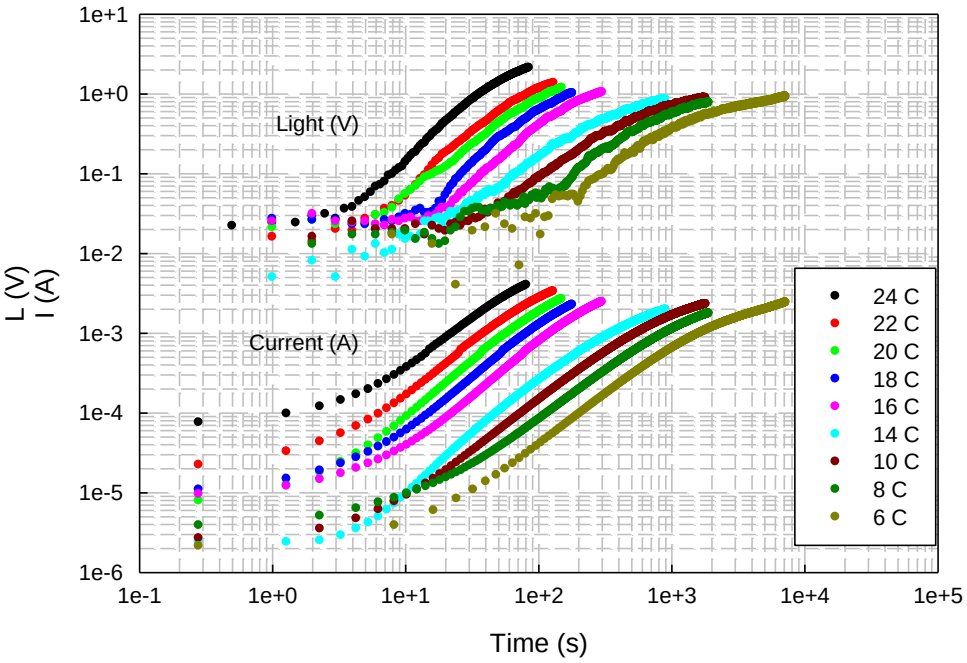

Figure 27. Current and Light Output as a Function of Time Following Application of 15 V Bias for Red A.

Light emission is due to electron-hole recombination in the polymer, per either the ED or EC model. Thus, it makes sense that an increasing current density would correlate with an increasing light output. Decreasing temperature shifts the curves to the right, corresponding to a longer turn-on time, without changing the shape of the curves. The longer turn-on times at lower temperatures are consistent with slower ion motion at lower temperatures.

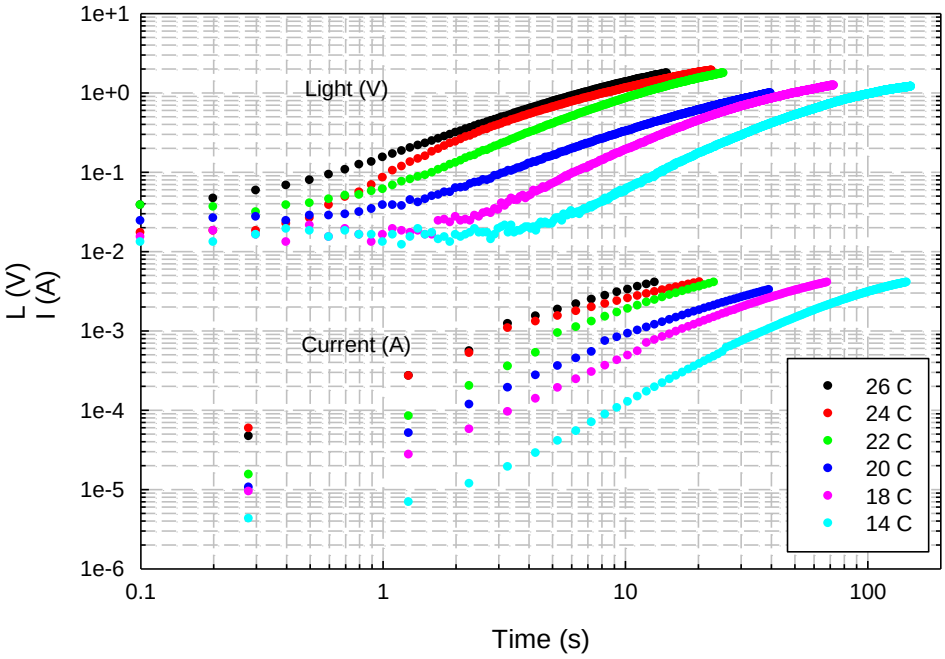

Figure 28. Current and Light Output as a Function of Time Following Application of 15 V Bias for Red B.

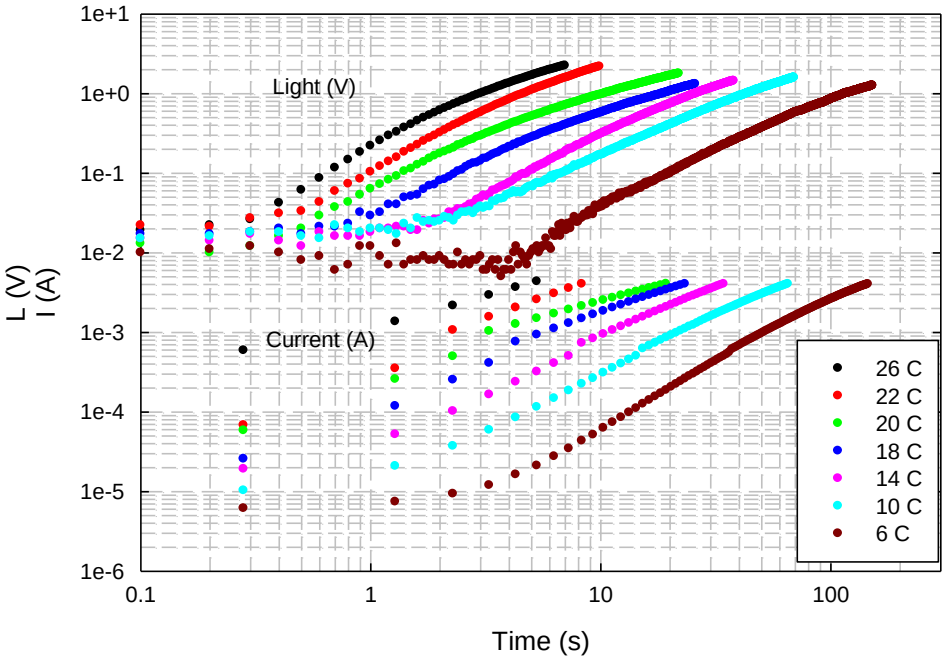

Figure 29. Current and Light Output as a Function of Time Following Application of 15 V Bias for Yellow B.

D. TEMPERATURE DEPENDENCE OF CAPACITANCE

As previously mentioned, transient current and light output of LECs have been reported and discussed in earlier works. This thesis presents the first transient measurements of capacitance as a function of temperature and bias voltage. Campbell *et al.* presented steady state capacitance measurements of an LEC before and after application of voltage [10]. We find, however, that in our devices capacitance continued to change under constant bias voltage for very long periods of time and did not reach or maintain a true steady state. This is clearly seen in Figures 30, 31 and 32, which show the transient capacitance for all three devices.

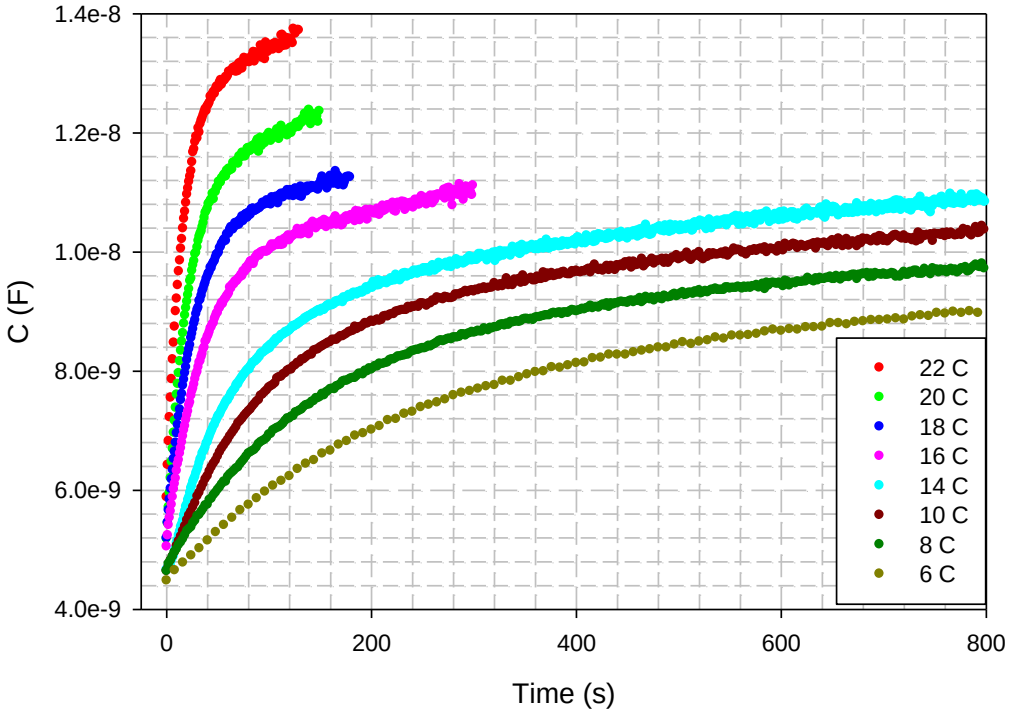

Figure 30. Capacitance as a Function of Time Following Application of 15 V Bias for Red A.

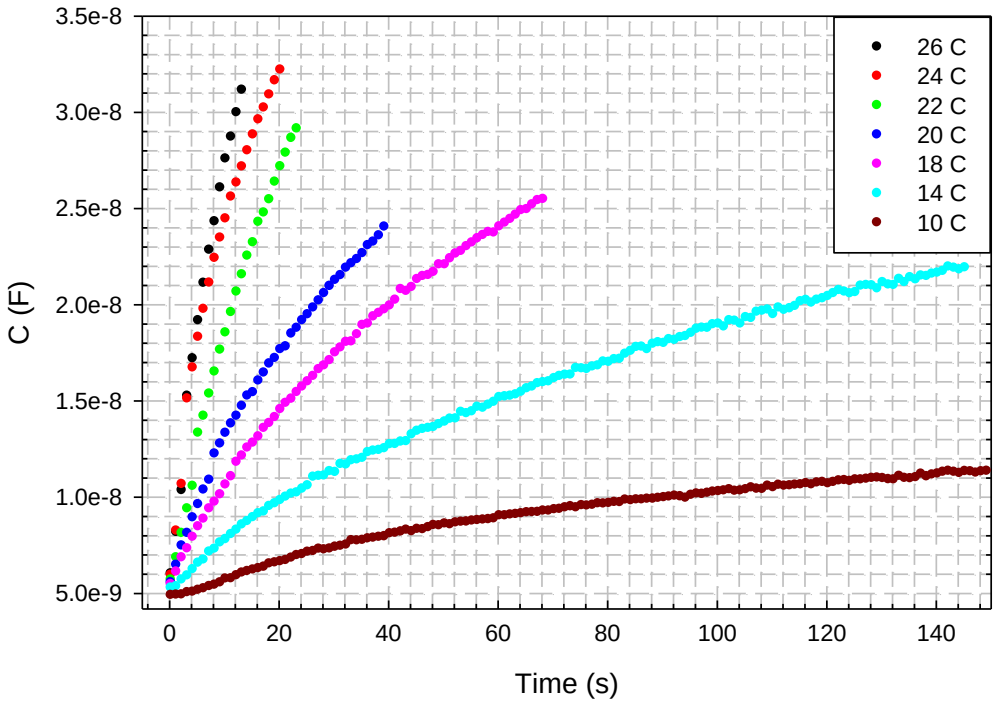

Figure 31. Capacitance as a Function of Time Following Application of 15 V Bias for Red B.

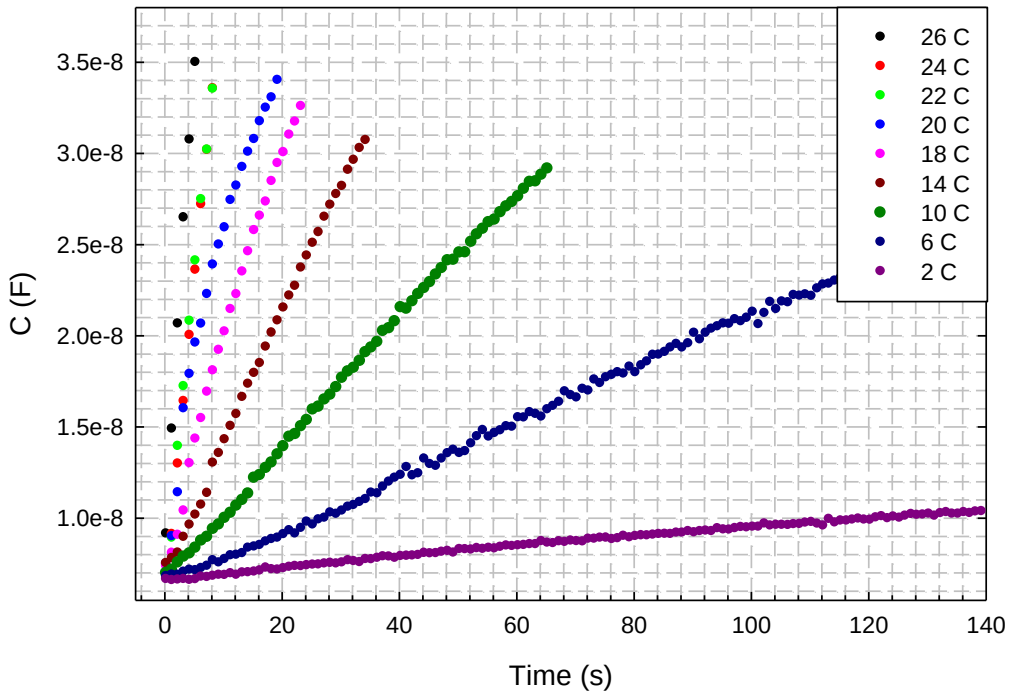

Figure 32. Capacitance as a Function of Time Following Application of 15 V Bias for Yellow A.

The change in capacitance is associated with the dynamic junction forming inside the LEC. We will think of the LEC as a parallel plate capacitor of area *A*, thickness *d*, and permittivity ε so that:

$$C = \frac{\varepsilon A}{d} \tag{12}$$

The electrodes of the LEC are the parallel plates and the PPV-PEO polymer blend of the LEC is the dielectric material between the plates, thus ε is the permittivity of the PPV-PEO. Since we observe a change in C at least one of these variables must be changing. Since *A* is constant at 1 cm^2, ε and/or *d* must change with time. The polymer layer is ~500 nm thick, but the effective *d* could vary depending upon the field distribution.

An increase in C correlates to an increase in ε, a decrease in *d*, or some combination of the two. Recalling the EC model, Figure 33, a decrease in *d* would suggest the insulating undoped junction region is shrinking, as the heavily doped p- and n- regions grow into the bulk due to ions accumulating on either side.

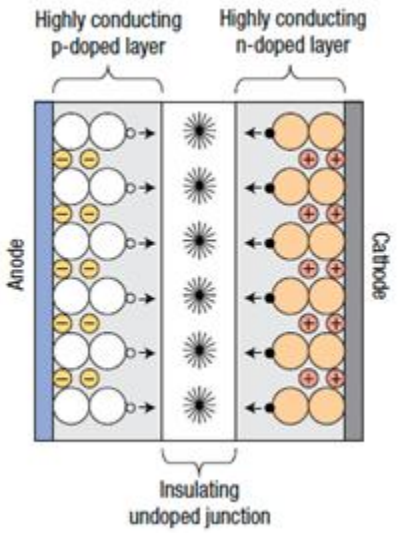

Figure 33. EC Model of P-N Junction Formation [From 6].

An increase of ε can also be attributed to a redistribution of the ions. Permittivity is determined by a material's ability to polarize in response to an electric filed. More ions exist in solution of the PEO at higher temperatures, and therefore we see a greater change in capacitance at higher temperatures.

The strong temperature dependence of the transient capacitance indicates a thermally activated process, or Arrhenius type behavior. Inside the LEC this process, called ion hopping, is an ion moving from point A to point B through the PEO. There is a potential energy (U) barrier, or activation energy, associated with the PEO that the ion must overcome in order to move, as shown in Figure 34.

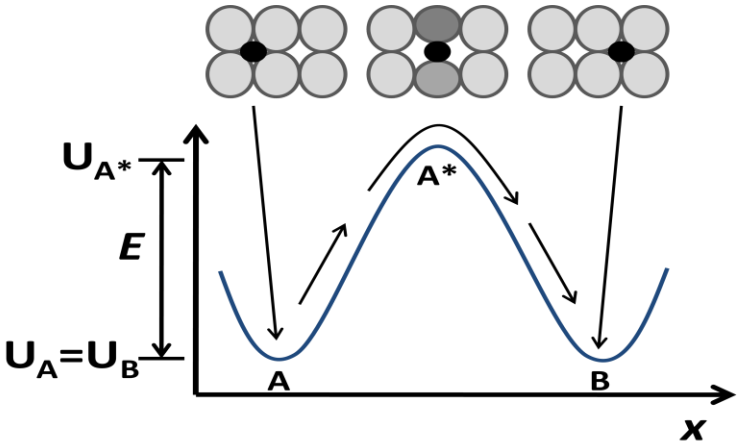

Figure 34. Activation Energy (*E*) of Ion Hopping in PEO.

The temperature dependence of ion hopping is given in Equation 13.

$$rate\ of\ \ change = Ae^{-E/kT} \tag{13}$$

Taking the rate of change to be *d*C/*d*t:

$$\log \frac{dC}{dt} = -\left(\frac{E}{k}\right)\left(\frac{1}{T}\right) + \log A \tag{14}$$

We took the initial slopes *d*C/*d*t from Figure 32, applied (13) and (14) and found a linear slope in the Arrhenius plot, Figure 35. The linear slope validates the theory of ion hopping with an activation energy $E \cong 1.27eV$.

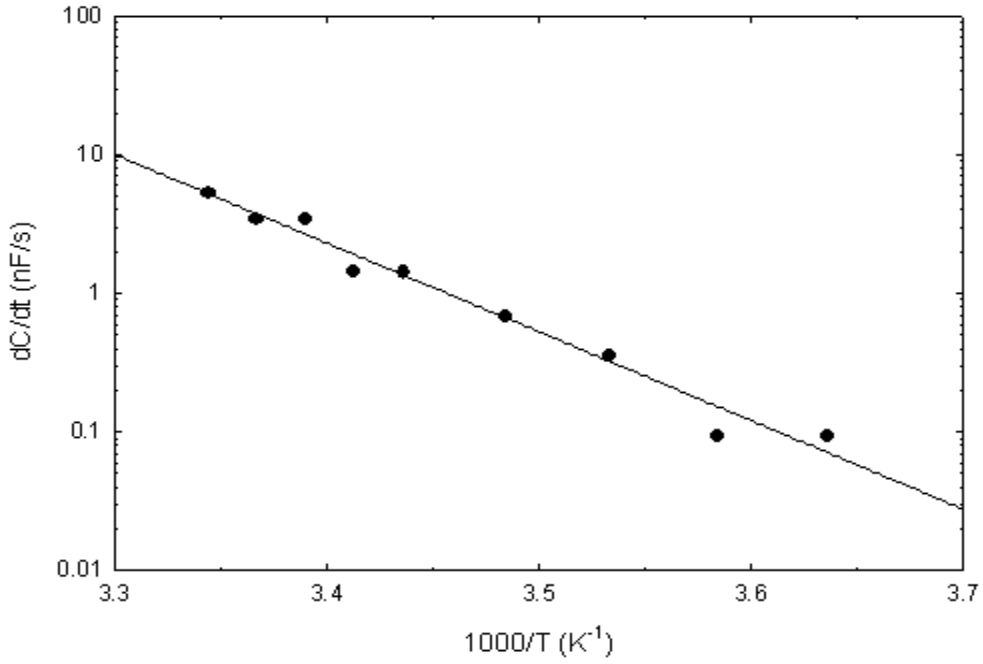

Figure 35. Arrhenius Plot of Rate of Change of Capacitance as a Function of Inverse Temperature for Yellow A.

E. RELATING CAPACITANCE, CURRENT AND LIGHT OUTPUT

We observed that transient light output, current and capacitance all increased during the turn-on time of the LEC. The data were acquired simultaneously during each experiment. In order to analyze the relationship between all three behaviors we normalized the initial and final measured values of current, light output and capacitance and plotted all three together as a function of time. These are shown in Figure 36 (Red A at 10°C), Figure 37 (Red B at 10°C) and Figure 38 (Yellow A at 2°C).

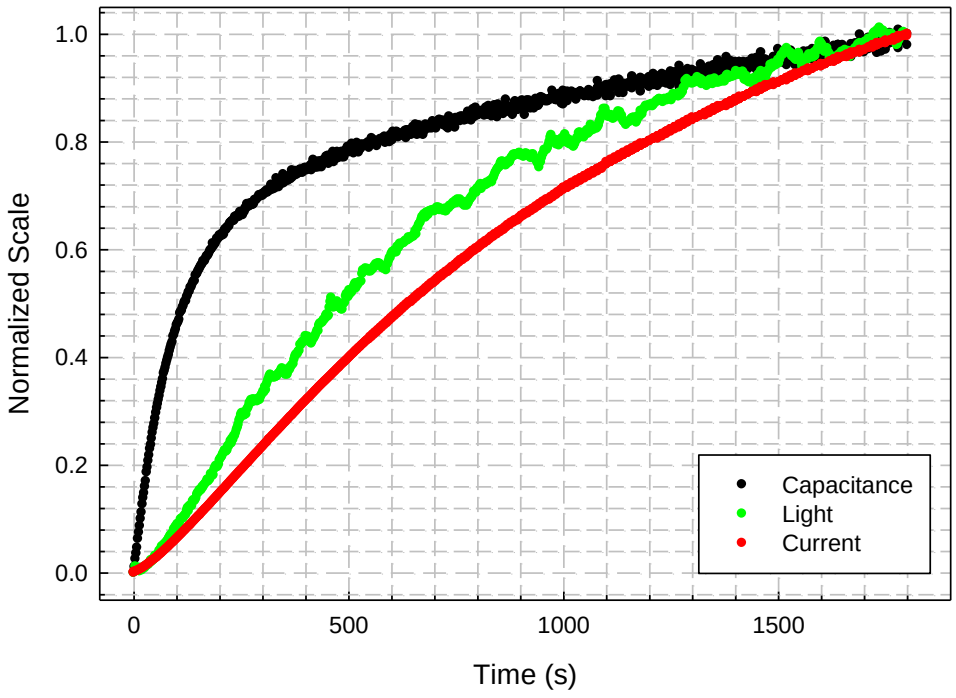

Figure 36. Normalized Change in C, L and I as a Function of Time for Red A at 10°C.

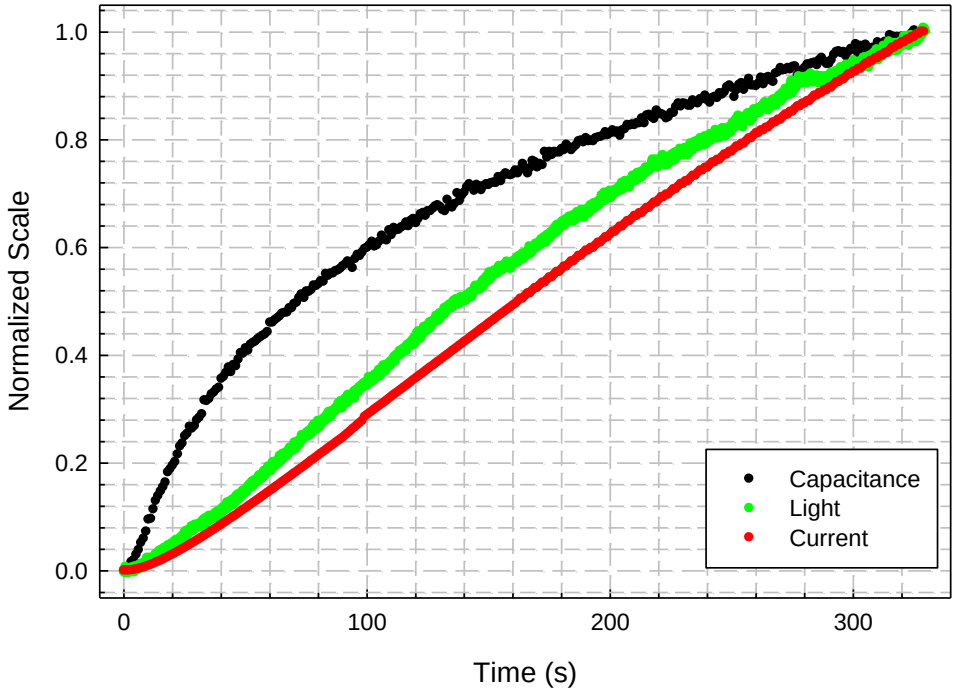

Figure 37. Normalized Change in C, L and I as a Function of Time for Red B at 10°C.

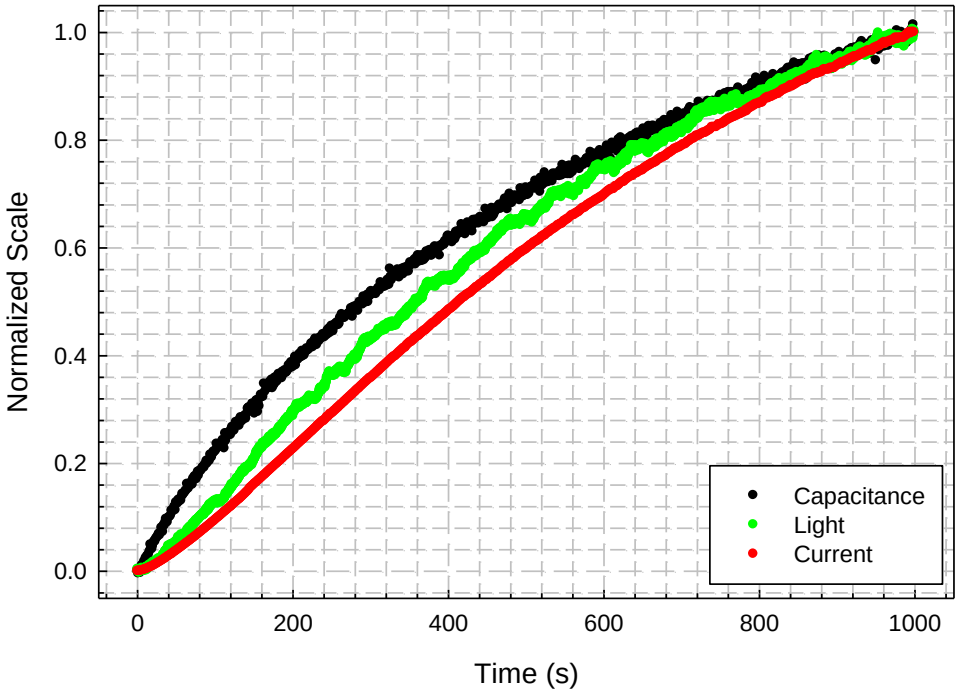

Figure 38. Normalized Change in C, L and I as a Function of Time for Yellow A at 2°C.

In each case, we observed that the change in capacitance *leads* the increase in current and light output (i.e., the initial rate of change is greatest for C), indicating that the junction forms prior to light emission and that ion motion does in fact enable the increased current injection under bias and the resulting light emission.

THIS PAGE INTENTIONALLY LEFT BLANK

V. VOLTAGE DEPENDENT MEASUREMENTS

A. LEC TURN-ON TRANSIENTS

After completing temperature dependent measurements, transient capacitance measurements were also made as a function of applied bias voltage. Again, all LECs used in the following experiments were third-generation devices. Two different LECs were used, both of which emitted primarily in the visible yellow: ID#24436b (Yellow 6b) and ID#24435b (Yellow 5b). While experiments were conducted on both devices, Yellow 5b was used and analyzed more extensively.

Burnett's work [4] showed that current and light output increased with time under constant bias voltage, but capacitance was not measured. Also, his data were collected over a relatively short time period, on the order of three seconds. Our goal was to measure the transient capacitance, current, and light output over the entire turn-on period of the devices. In order to extend this turn-on time, all experiments were conducted at a temperature of 15°C. Initial experiments suggested that the devices required a threshold bias voltage to turn on, around 8-10 V, so a bias voltage range from 6 V to 17 V was selected.

B. VOLTAGE DEPENDENCE OF CURRENT

We expected the current to increase during the turn-on time, and again imposed the 4 mA maximum current in order to protect the devices. Results for the two devices are shown in Figure 39 and Figure 40. We observed that as bias voltage increased so did the initial *rate* of increase of current density. We also observed that the current density began to approach a steady state at lower bias voltages.

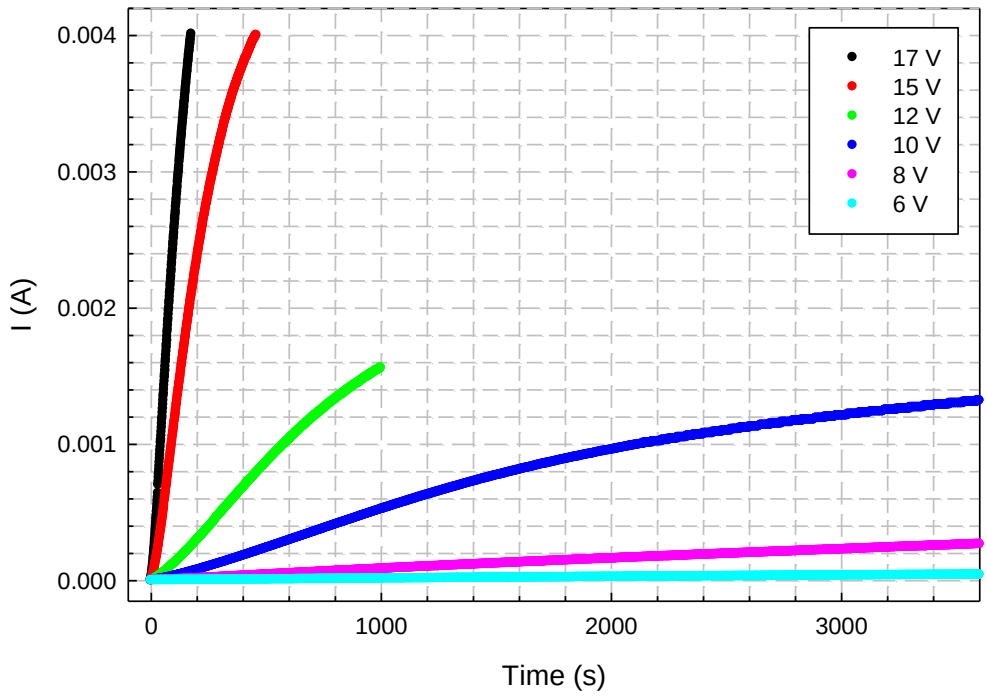

Figure 39. Current as a Function of Time Following Application of Different Bias Voltage for Yellow 6b. T = 15°C.

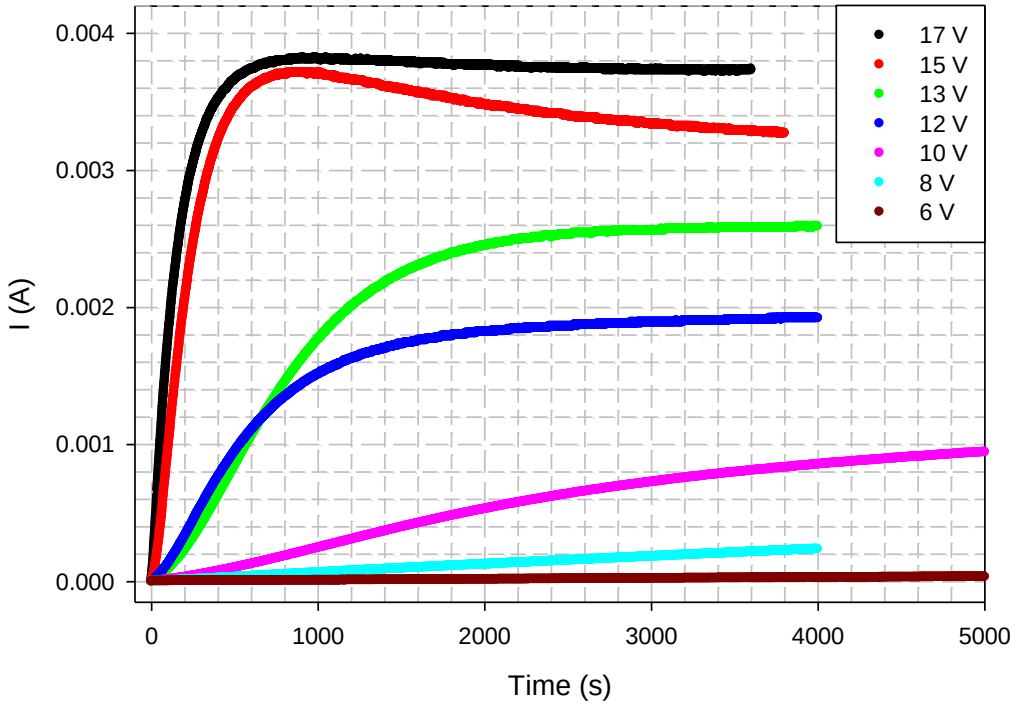

Figure 40. Current as a Function of Time Following Application of Different Bias Voltage for Yellow 5b. T = 15°C.

C. VOLTAGE DEPENDENCE OF LIGHT OUTPUT

We observed the same direct correlation between current density and light output as we did in the temperature dependent measurements: as current density increased the light output also increased. In fact, the transient light response, shown in Figures 41 and 42, looks nearly identical to the transient current response in Figure 39 and Figure 40, including the decrease at longer times for sample Yellow 5b.

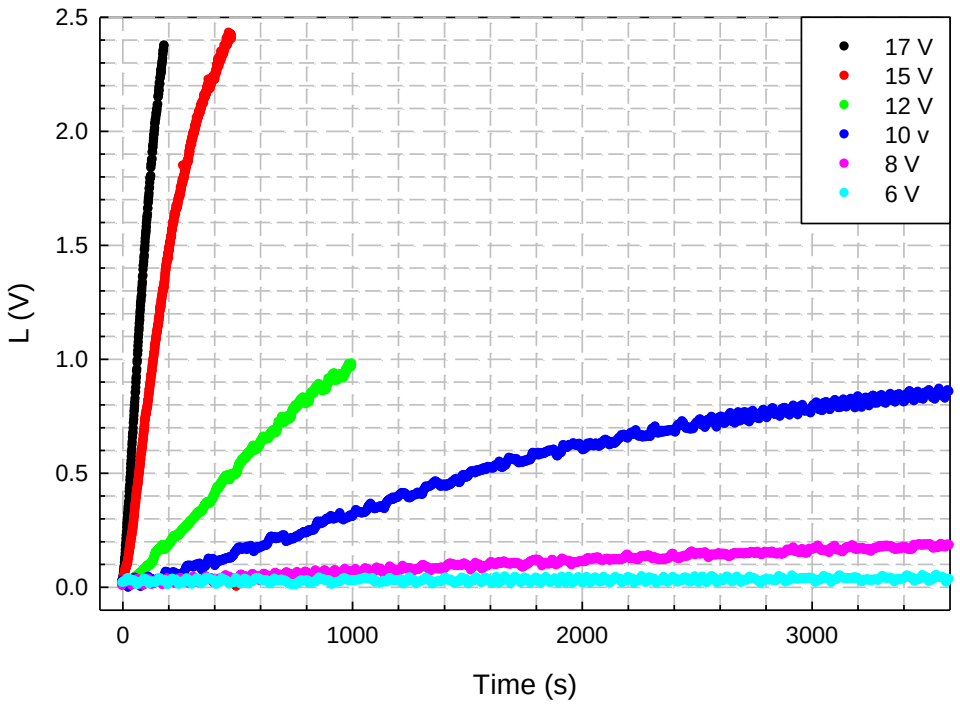

Figure 41. Light Output as a Function of Time Following Application of Different Bias Voltage for Yellow 6b. T = 15°C.

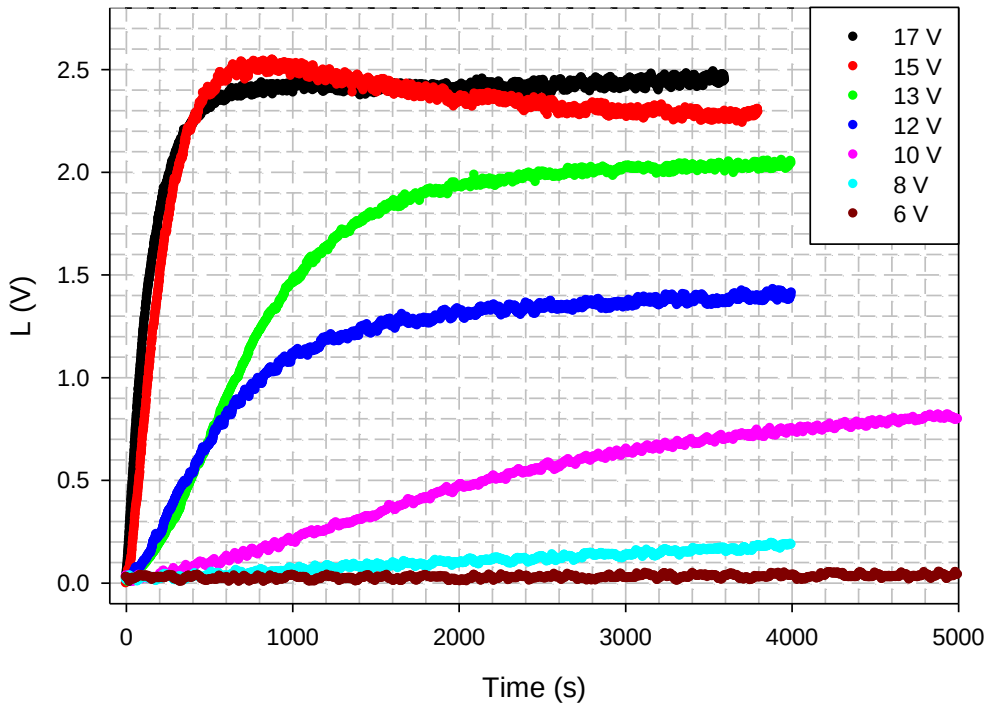

Figure 42. Light Output as a Function of Time Following Application of Different Bias Voltage for Yellow 5b. T = 15°C.

Light output was visible to the naked eye when the detector photo voltage was approximately 0.25 V. Within an hour, neither device emitted light visible to the naked eye when a bias voltage below 10 V was applied. The lack of light output below a certain bias voltage is due to insufficient current required for measurable photon emission. The low current means the electron and hole concentrations are too low for the device to function as an LEC, i.e., the junction is unable to fully form below a threshold voltage.

D. VOLTAGE DEPENDENCE OF CAPACITANCE

The transient response of the capacitance for the same range of applied voltages is shown in Figures 42 and 43. We observed that under constant bias voltage the capacitance initially increased, similar to the temperature dependent measurements. We also observed, however, that this initial increase at lower bias was relatively small, compared to the temperature dependent measurements, and that the rate of change of capacitance decreased over the turn-on time. At lower bias voltages the initial change in capacitance decreased. Although the rate of change continued to show a bias dependence, the actual ΔC appears to become independent of voltage at values below ~10 V, as shown in Figures 43 and 44.

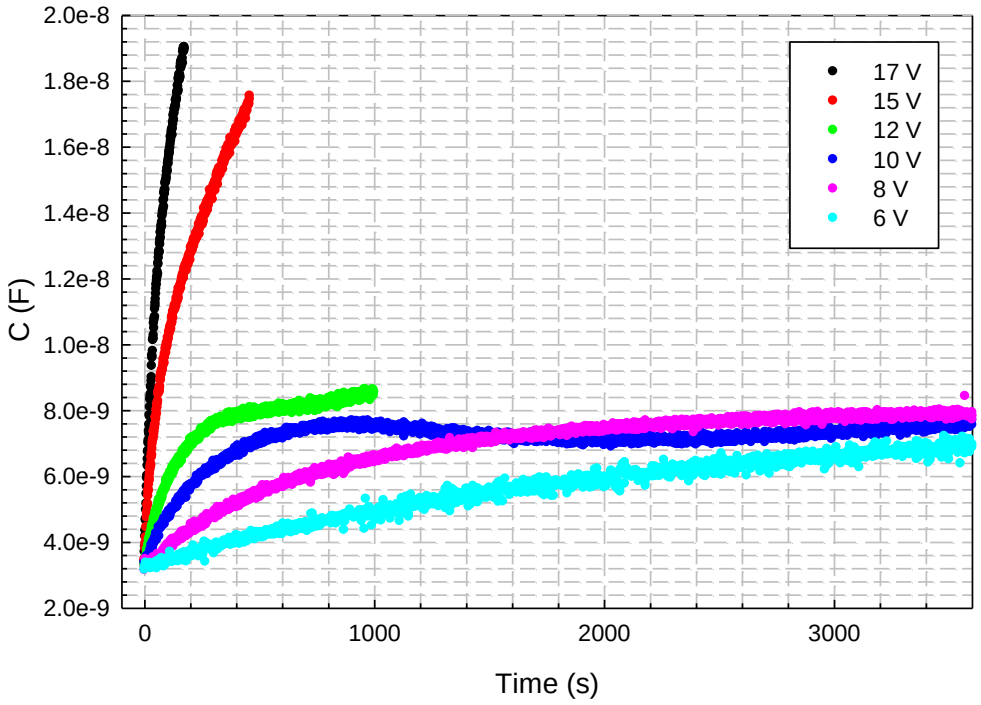

Figure 43. Capacitance as a Function of Time Following Application of Different Bias Voltage for Yellow 6b. T = 15°C.

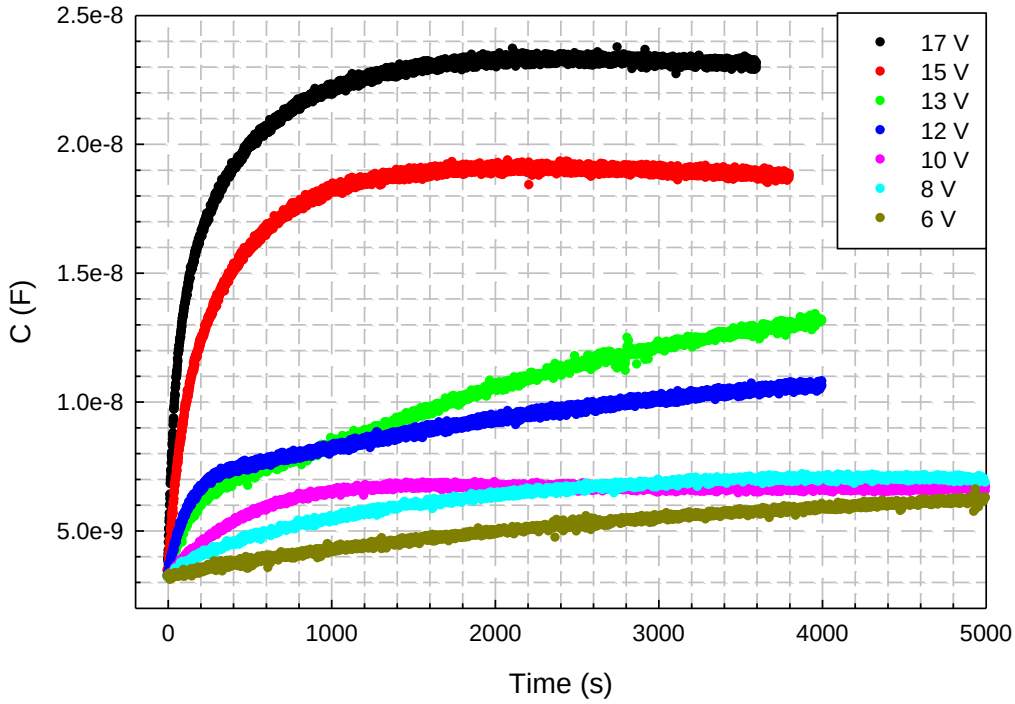

Figure 44. Capacitance as a Function of Time Following Application of Different Bias Voltage for Yellow 5b. T = 15°C.

As observed in the temperature dependent measurements, the capacitance never reaches a true steady state. It is interesting to note that in Yellow 5b the capacitance does reach a maximum, for 17 V and 15 V, and then begins to decrease slightly. In both devices, for bias voltages of 10 V and lower, capacitance is converging to relatively the same value. Figures 45 and 46 show the final capacitance values reached over the measured time period for Yellow 6b and Yellow 5b, respectively. The capacitance vs. bias voltage behavior indicates a threshold voltage associated with junction formation. A threshold voltage is necessary to establish a sufficient electric field within the LEC, which would then allow ion motion, electron/hole injection and thus the emission of light.

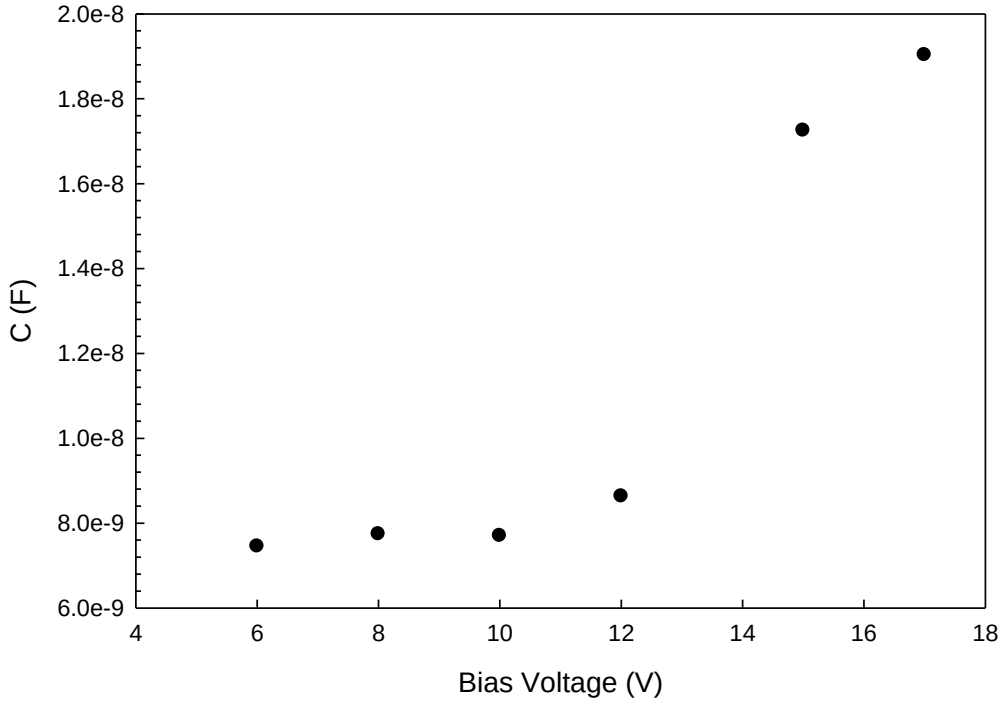

Figure 45. Final Capacitance Value as a Function of Bias Voltage for Yellow 6b.

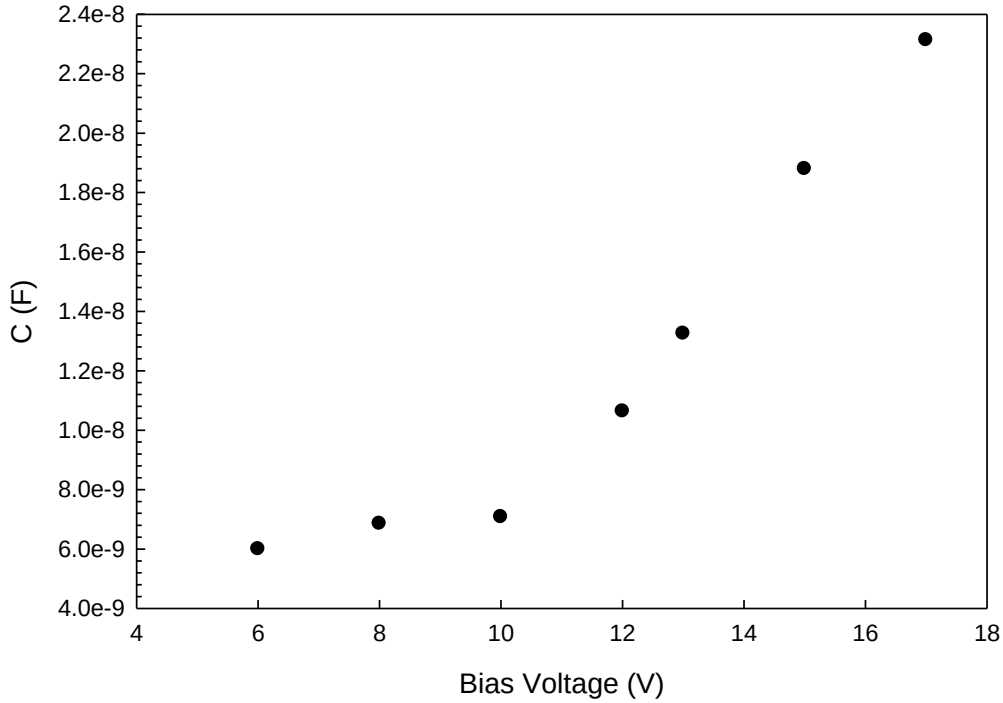

Figure 46. Final Capacitance Value as a Function of Bias Voltage for Yellow 5b.

Similar capacitance as a function of bias voltage results were reported by Campbell *et al.* [10], however their measurements were taken statically after applying the bias voltage for only 15 seconds and claiming this established a steady state within the LEC. Our transient measurements suggest that it is difficult to identify a true steady state in these devices.

E. RELATING CAPACITANCE, CURRENT AND LIGHT OUTPUT

We observed that transient light output, current and capacitance increased upon initial application of bias during the turn-on time of the LEC, but the rate of change (i.e., the slope) varied and indicated multiple transient phenomena. The current, light and capacitance data were acquired simultaneously during each experiment. In order to analyze the relationship between all three parameters we again normalized the current, light and capacitance for a given time period so that the end points coincided and plotted

all three together as a function of time. This comparison is shown in Figure 47 (Yellow 6b at 8 V) and Figure 48 (Yellow 5b at 8 V). The noise in the light, in both Figures 47 and 48, is due to the very low photo-voltage at 8V, though the increasing trend is still clearly present at such low levels of light output.

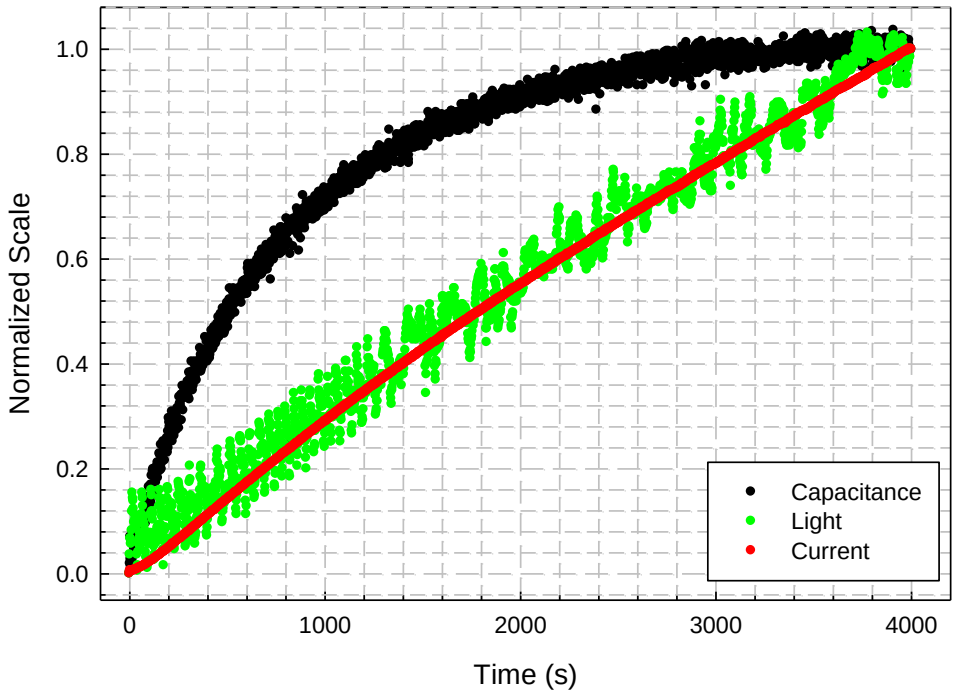

Figure 47. Normalized Change in C, L and I as a Function of Time for Yellow 6b at 8 V.

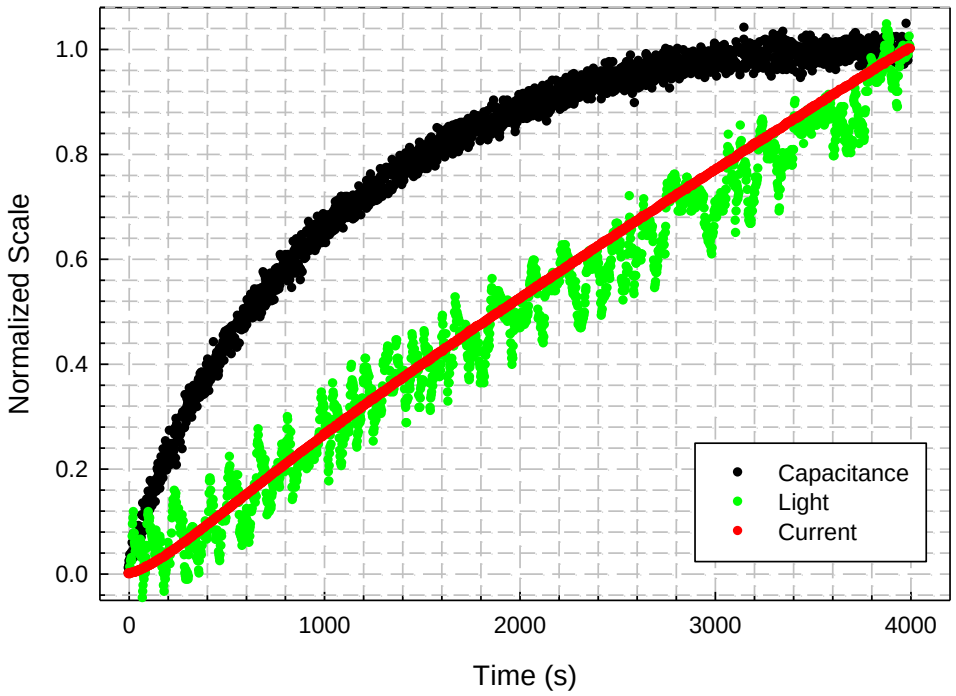

Figure 48. Normalized Change in C, L and I as a Function of Time for Yellow 5b at 8 V.

In each case, we again observed that the change in capacitance *leads* the increase in current and light output (i.e., the initial rate of change is greatest for C), indicating that the junction forms prior to light emission. This suggests that ion motion, which determines the capacitance change, changes the electric field profile to allow increased carrier injection and recombination. Campbell [10] also observed an increase in static capacitance as a function of bias voltage prior to an increase in current and asserts that the junction forms before sufficient current can flow to enable light emission.

By making the same measurements for Yellow 6b at a lower bias voltage (Figure 49), we find that light emission was not above the noise. The comparison between capacitance and current, however, shows the same behavior as at higher voltages.

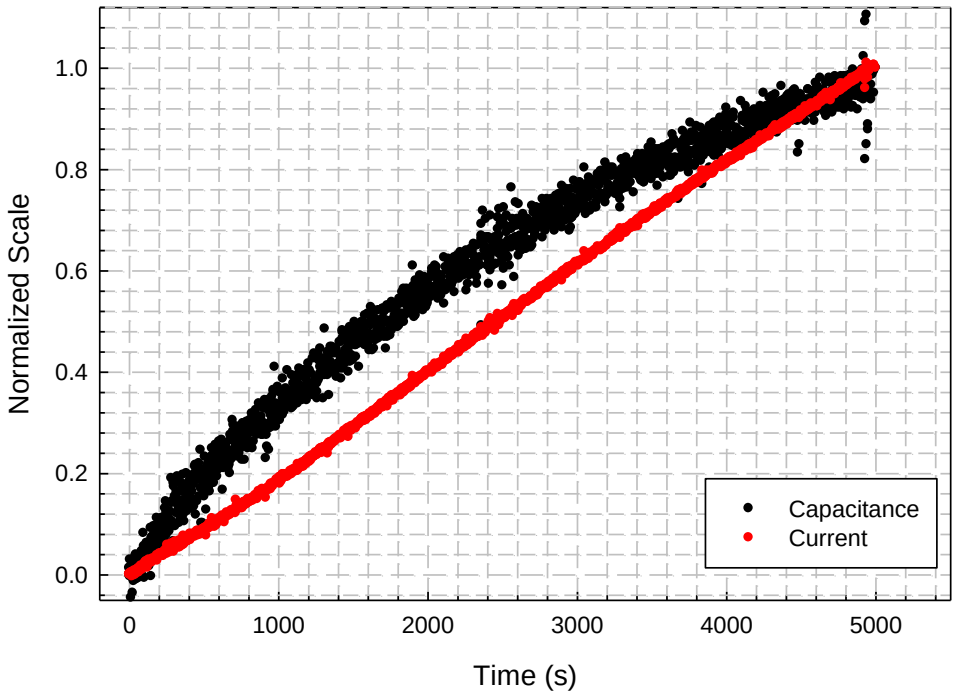

Figure 49. Normalized Change in C and I as a Function of Time for Yellow 5b at 6 V.

F. TRANSIENT BEHAVIOR AS A FUNCTION OF VOLTAGE AT 22°C

After examining the behavior in Figure 44, where the capacitance of Yellow 5b was observed to converge to relatively the same value for bias voltage less than 10 V, we conducted the same experiments at room temperature, 22°C. We hypothesized that the capacitance leveling behavior at the lower temperature, 15°C, was due to the smaller percentage of ions existing in solution available to assist in junction formation. At a higher temperature more of the salt ions would disassociate, causing more cations and anions to be available and thus the capacitance would increase. However, this behavior was not observed over the measured range of bias voltage.

The lower bias, however, allowed for measurement of the capacitance over a much longer time scale. This is shown, for biases from 2 V to 6 V, in Figure 50. The oscillating behavior of the capacitance was not expected, nor is it well understood. A

possible explanation is that there is a neutralization of ion charge over time. We again compared this new capacitance behavior of Yellow 5b with the corresponding current and light output by normalizing each and plotting all three together as a function of time, which is shown in Figures 51 (5 V bias) and 52 (4 V bias).

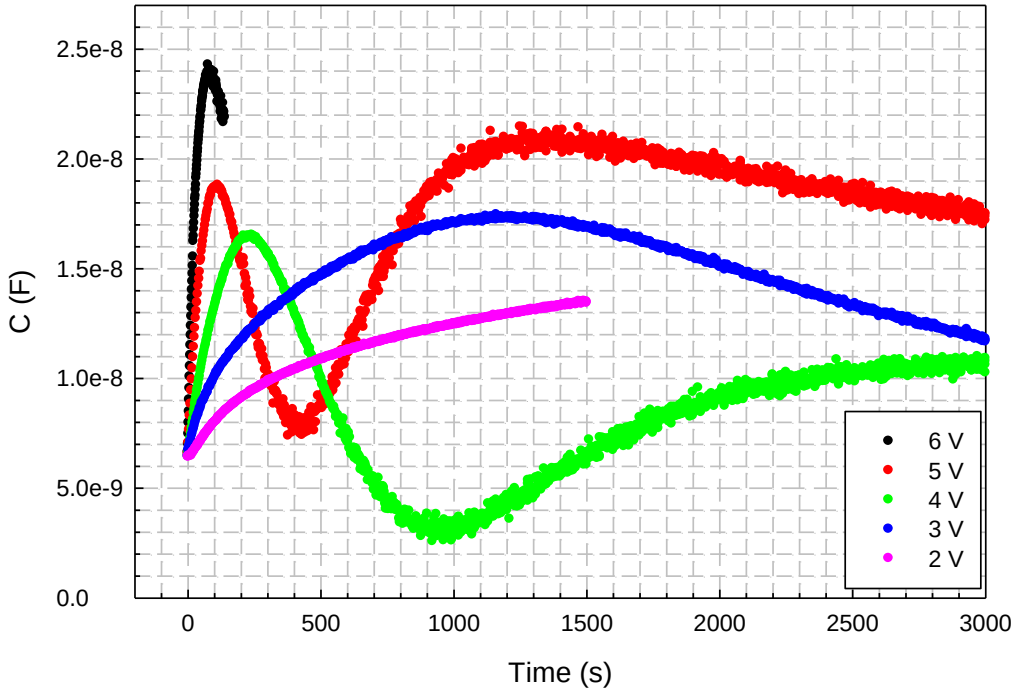

Figure 50. Capacitance as a Function of Time Following Application of Different Bias Voltage for Yellow 5b at 22°C.

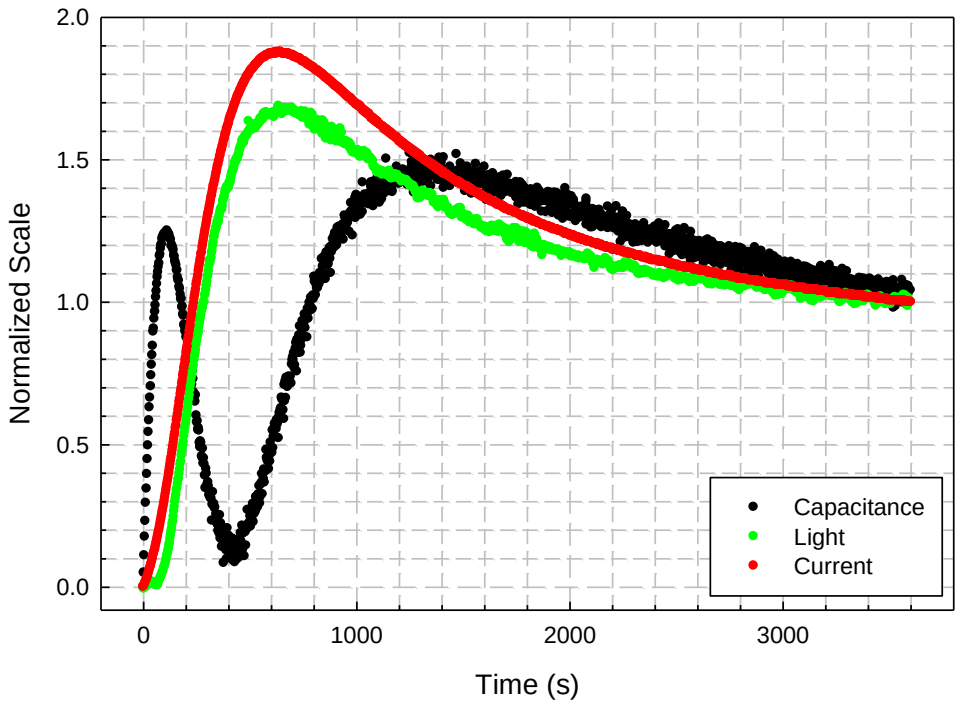

Figure 51. Normalized Change in C, L and I as a Function of Time for Yellow 5b with 5 V at 22°C.

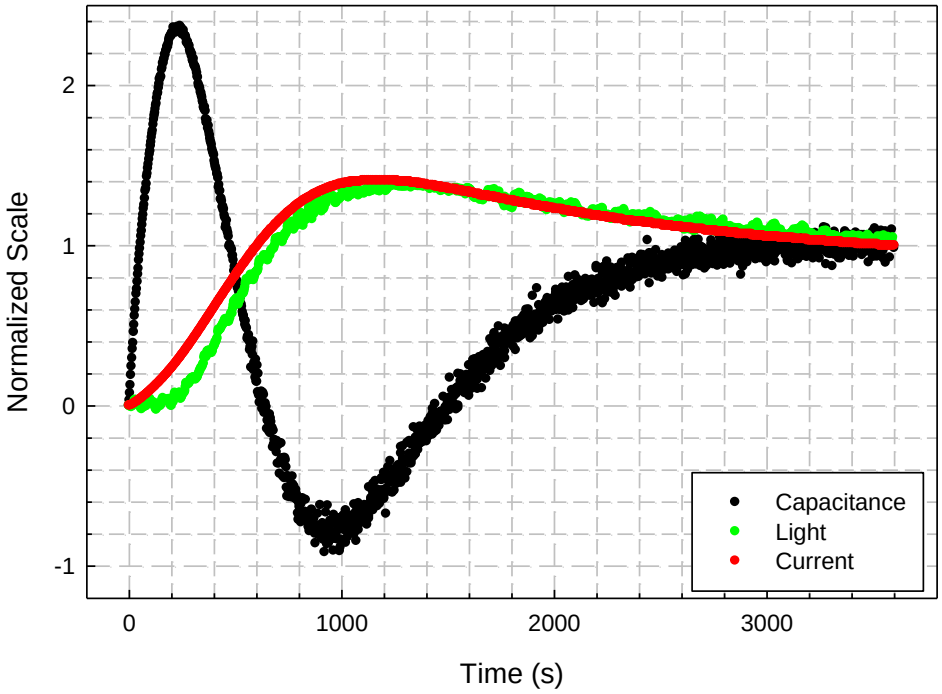

Figure 52. Normalized Change in C, L and I as a Function of Time for Yellow 5b with 4 V at 22°C.

It is interesting to note that the minimum capacitance value occurs slightly before the current and light output reach a maximum in both cases. This transient capacitance behavior is a topic for future analysis.

THIS PAGE INTENTIONALLY LEFT BLANK

VI. CONCLUSIONS AND SUGGESTIONS FOR FURTHER RESEARCH

A. SUMMARY OF RESULTS

In this work, the transient behavior of an LEC was studied as a function of temperature and bias voltage. The focus was on the transient capacitance behavior during the dynamic junction formation in an LEC. These are the first transient measurements of capacitance of an LEC. Whether under varying temperature or varying bias voltage conditions the *initial* change in capacitance increases monotonically, but the rate of change is strongly dependent on both temperature and bias voltage.

Temperature dependence measurements at constant bias voltage suggest a thermally activated process is associated with the junction formation, namely ion hopping within the PEO. An activation energy of 1.27 eV was found for the PEO. Voltage dependence measurements at 15°C suggest there is a minimum bias voltage required to establish junction formation and enable light emission. The voltage dependence measurements taken at room temperature require further analysis to understand the decreasing and oscillatory behavior of the transient capacitance.

The parameter space for experiments on LECs is extremely complex. We showed that, under 15 V bias, changing the temperature scale by only a few degrees resulted in orders of magnitude changes in the time scale of junction formation. This means that the time scales to observe different parts of the transient behavior vary greatly as a function of operating parameters. Although this work focused on the first comprehensive measurements of initial transient capacitance behavior, a variety of longer term phenomena (e.g., decreasing capacitance at longer times) were also observed for the first time. These results will stimulate further development of the theory of ion motion and electric field distribution in LEC devices.

B. SUGGESTIONS FOR FURTHER RESEARCH

Copious amounts of data were collected during this research and the limited time frame did not allow for full analysis. This raw data includes transient resistance as well as transient capacitance as a function of frequency. Analyzing the capacitance change as a function of frequency could provide insight into the impact of, and allow for the isolation of, ion motion during the dynamic junction formation.

The turnover and oscillatory capacitance behavior measured at 22°C is very interesting and has never been previously observed. Analysis of this behavior could provide insight into the change in capacitance due to the changing permittivity of the polymer and/or the changing thickness of the junction in time.

LIST OF REFERENCES

[1] R. Pengelley, "Cutting through the fog of war: armed forces strive to reduce fratricide threat," International Defense Review, 01 May 2006

[2] "FY09 Technology Transition Initiative Projects" from Office of Secretary of Defense website, retrieved May 18, 2010, http://www.acq.osd.mil/ott/tti/FY09projects.htm.

[3] Q. Pei and F. Klavetter, "Electrochemical light-emitting devices," U.S. Patent 5682043, June 28, 1994.

[4] K. Burnett, "Low temperature transient performance of a polymer light-emitting diode," M. S. thesis, Naval Postgraduate School, Monterey, CA, 2010.

[5] Q. Pei, G. Yu, C. Zhang, Y. Yang, and A. J. Heeger, "Ploymer light-emitting electrochemical cells," *Science,* vol. 269, p. 1086, 1995.

[6] J. C. deMello, "What's in a name?" *Nat. Mat*., vol. 7, p. 796, 2007.

[7] Q. Pei, G. Yu, C. Zhang, Y. Yang, and A. J. Heeger, J., "Polymer light-emitting electrochemical cells: in situ formation of a light-emitting p-n junction," *Am. Chem. Soc.,* vol. 118, p. 3922, 1996.

[8] D. J. Dick, A. J. Heeger, Y. Yang, and Q. Pei, "imaging the structure of the p-n junction in polymer light-emitting electrochemical cells," *Adv. Mat*., vol. 8, p. 985, 1996.

[9] D. L. Smith, "Steady state model for polymer light-emitting electrochemical cells," *J. Appl. Phys.*, vol. 81, p. 2869, 1997.

[10] I. H. Campbell, D. L. Smith, C. J. Neef, and J. P. Ferraris, "Capacitance measurements of junction formation and structure in polymer light-emitting electrochemical cells," *Appl. Phys. Lett*., vol. 72, p. 2565, 1998.

[11] J. C. deMello, N. Tessler, S. C. Graham, and R. H. Friend, "Ionic space charge effects in polymer light-emitting diodes," *Phys. Rev. B.,* vol. 57, p. 12951, 1998.

[12] J. D. Slinker *et al.*, "Direct measurement of the electric-field distribution in a light-emitting electrochemical cell," *Nature Mater*., vol. 6, p. 894, 2007.

[13] L. S. C. Pingree, D. B. Radovsky, D. C. Coffey, G. P. Bartholomew, and D. S. Ginger, "Scanning kelvin probe imaging of the potential profiles in fixed and dynamic planar LECs," *J. Am. Chem. Soc*., vol. 129, p. 15903, 2007.

[14] S. Reenen, P. Matyba, A. Dzwilewski, A. J. Janssen, L. Edman and M. Kemerink, "A unifying model for the operation of light-emitting electrochemical cells," *J. Am. Chem. Soc.*, vol. 132, p. 13776, 2010.

[15] L. Edman, M. A. Summers, S. K. Barratto, and A. J. Heeger, "Polymer light-emitting electrochemical cells: Doping, luminescence, and mobility," *Phys. Rev. B.*, vol. 70, p. 115212, 2004.

INITIAL DISTRIBUTION LIST

1. Defense Technical Information Center
   Ft. Belvoir, VA

2. Dudley Knox Library
   Naval Postgraduate School
   Monterey, CA

3. Professor Andres Larraza
   Naval Postgraduate School
   Monterey, CA

4. Professor Peter P. Crooker
   Naval Postgraduate School
   Monterey, CA

5. Professor Nancy M. Haegel
   Naval Postgraduate School
   Monterey, CA

6. LT Yevtte A. Davis
   Naval Postgraduate School
   Monterey, CA

7. Dr. Devin Mackenzie
   Director of Technology
   Add-Vision, Inc.
   Scotts Valley, CA